Journal of Environmental Management 231 (2019) 524–545

Contents lists available at ScienceDirect

Journal of Environmental Management

journal homepage: www.elsevier.com/locate/jenvman

Research article

Evidence of climatic change in Vietnam: Some implications for agricultural production

Kien Nguyen Duc[a,b,*], Tiho Ancev[b], Alan Randall[b,c]

[a] Faculty of Economics and Development Studies, University of Economics, Hue University, 99 Ho Dac Di Street, Hue City, Viet Nam
[b] School of Economics, The University of Sydney, Sydney, NSW, 2006, Australia
[c] Environmental & Development Economics, The Ohio State University, Columbus, OH, OH 43210, USA

ARTICLE INFO

Keywords:
Climate change
Spatio-temporal pattern
Statistical methods
Geostatistical techniques
Farming
Vietnam

ABSTRACT

Systemic changes in environmental conditions, such as climate, can have a significant impact on both natural and human systems. This paper provides an improved understanding of the spatio-temporal variations in underlying climate processes, and the potential effects climate change may have on Vietnam's agricultural sector. Statistical methods were combined with geostatistical techniques to test the statistical significance of long-term trends in the climatic variables, graphically representing the distribution of climate patterns, identifying variations and trends of changes over time and their likely effects on agricultural production. By using records of monthly precipitation and temperature for a relatively long-term period (1975–2014) over a high density of 112 meteorological stations across the country, robust statistical and visual evidence of climatic change throughout Vietnam are provided. The Mann-Kendall trend test confirms the statistically significant long-term trends of rainfall and temperature in many regions across the country. The visual analysis shows remarkable changes in the spatio-temporal distribution patterns of those variables and most of the 'hotspot' areas identified by geostatistical mapping are in areas with confirmed long-term trends. The long-term significant trends are also concentrated in areas with very high proportion of agricultural land, particularly land used for rice production in the Red River and Mekong River deltas. The findings deliver a better understanding of underlying climate processes and impacts across regions of Vietnam and provide a basis to develop effective climate-related policies for agricultural production in response to changing climatic conditions.

1. Introduction

Climatic conditions are changing across the globe but vary in direction, frequency, and intensity by location. The Intergovernmental Panel on Climate Change notes that globally averaged surface temperature showed an increasing linear trend of 0.85 °C between 1880 and 2012 (Stocker et al., 2014). It is also very likely that extreme weather events have increased in frequency and intensity on a global and local scale (Caesar et al., 2011; Pingale et al., 2014). In Vietnam, from the 1970s the recorded average temperature has increased by 0.26 ± 0.10 °C per decade, twice the rate of global warming for the same period (Nguyen et al., 2013). Total annual rainfall is dominated by a negative trend in five out of eight climatic zones of Vietnam (Nguyen et al., 2013). Changes in climate have also intensified the incidence and magnitude of extreme events such as floods, droughts, and typhoons. It has been estimated that climatic change may directly affect the livelihoods of about 10–12% of Vietnam's population and lead to the loss of approximately 10% of Gross Domestic Product (VNGP, 2011). Furthermore, the country's most climate-dependent activity – agricultural production – still dominates Vietnam's economy, accounting for 22% of GDP and 54% of the labor force (GSO, 2014).

A better understanding of the pattern of climatic variability and change at various spatial and temporal scales is crucial to provide rigorous evidence-based information to policy-makers at all levels in the decision-making process and to guide the development and implementation of appropriate adaptation responses (Conway et al., 2015; Nam et al., 2016). At the global and regional scales, a substantial number of studies have investigated and documented the changing patterns of climatic variables across space and time (Kundu et al., 2015; Nam et al., 2016; Portmann et al., 2009; Río et al., 2011; Stocker et al., 2014). However, most previous studies have concentrated either on testing the spatial and temporal trends in climate-related variables using statistical trend analysis methods such as the Mann-Kendall and Spearman rho tests (Jaiswal et al., 2015; Pingale et al., 2014; Xu et al.,

* Corresponding author. Faculty of Economics and Development Studies, University of Economics, Hue University, 99 Ho Dac Di Street, Hue City, Viet Nam.
E-mail address: ndkien@hce.edu.vn (K. Nguyen Duc).

https://doi.org/10.1016/j.jenvman.2018.10.011
Received 10 April 2018; Received in revised form 3 October 2018; Accepted 4 October 2018
Available online 26 October 2018
0301-4797/ © 2018 Elsevier Ltd. All rights reserved.

2018) or on assessing the patterns of climatic change using geostatistical techniques (Chen and Guo, 2017; Conway et al., 2015; Javari, 2017; Mustafa et al., 2007). Consequently, little attention has been paid thus far to simultaneously investigating the relationship between trends and spatial pattern changes in meteorological elements and relating evidence of climate change to impacts on human socio-economic activities. For instance, Río et al. (2011) combined statistical testing and geostatistical techniques to investigate the spatial distribution of rainfall trends in Spain from 1961 to 2006. Their study demonstrates the advantage of combining statistical trend analysis methods and spatial interpolation techniques to detect trends and using visualization techniques to improve the spatio-temporal interpretation of detected trends. However, connections between human activity and climate change were beyond the scope of their study.

For the case of Vietnam, there are a very limited number of studies investigating the spatial and temporal patterns of climatic change and its impact using local scale data (Caesar et al., 2011; Griffiths et al., 2005; Lau and Yang, 1997; Nguyen et al., 2007, 2013). Recently, a notable attempt of Nguyen et al. (2013) contributed to explaining the changes in climate across regions of Vietnam using the Mann-Kendall trend test and they found a continuing increase in average temperature and adverse trends of rainfall variability in various sub-regions. However, because their study has a national and regional focus, further analysis using disaggregated local weather station-level data is required to reduce the bias caused by data aggregation in climate research (Rulfová and Kyselý, 2013; Zhao et al., 2015). Our study combines statistical testing and geostatistical techniques (Río et al., 2011) with application to Vietnam using highly disaggregated weather station data. We also add to the current state-of-the-art by including more climatic variables measured at the local scale, and by examining the exposure of rice cultivation across the country to the effects of climate trends and changes in weather pattern. To the best of our knowledge, this study is among very few empirical studies globally that apply both statistical tests and geostatistical techniques to examine spatio-temporal evidence of climatic change and identify its impact in agriculture using land-based observations, and certainly is the first such study for Vietnam.

We make several contributions to the literature. One is by analyzing long-term, spatio-temporal changes in climatic patterns, and establishing the nature of adverse impacts of climatic variation on climate-exposed production sectors, such as agriculture. Another is by integrating statistical and geostatistical techniques, which allows us to provide new evidence of ongoing climate change, both temporally and spatially, and capture the complex distribution of climatic elements using long-term weather station records of meteorological data and a higher density of land-based weather stations across Vietnam. The comprehensive approach of combining statistical testing with geostatistical techniques enables mapping of climate patterns at a very fine resolution to identify changes and trends over time and statistically confirm their significance. The non-parametric trend test confirms the presence of long-run trends of climatic variables, providing evidence of ongoing climate change. Use of mapping techniques confirms the evidence of climatic change and highlights its spatial dimension, spatially relating observed climate change to land use and agricultural production. We then link the empirical statistical and visual evidence of the spatio-temporal variations of climatic conditions to rice production throughout Vietnam to identify potential impact. In doing so, we provide robust evidence of the potential impact of climatic change on rice cultivation across regions of Vietnam. Given the recently observed significant changes in climate conditions, it is reasonable to expect more negative climate-related consequences for agriculture due to the sector's direct exposure to the variations of climatic elements.

The paper is structured as follows. The next section provides an overview of the study area and the data used in this study. Section 3 describes the research workflow and methods applied, and the empirical findings are discussed in Section 4. Section 5 provides some concluding remarks.

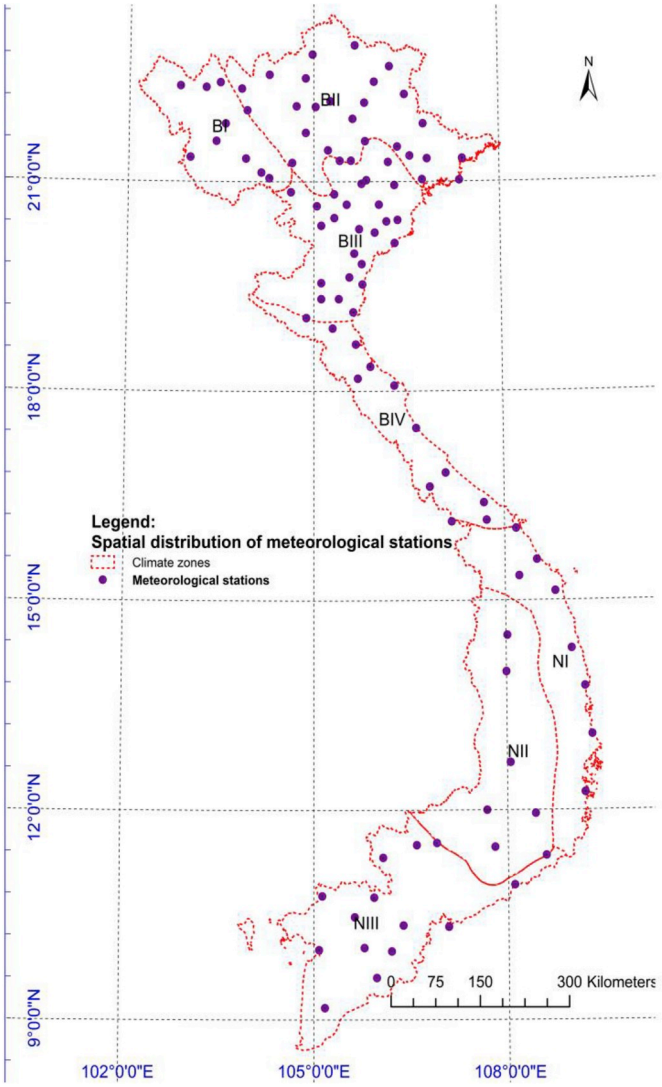

Fig. 1. Spatial distribution of 112 meteorological stations and climate zones in Vietnam.

2. Study area and data

2.1. Study area

Located in the tropical zone of the Northern Hemisphere, Vietnam is characterized by a tropical monsoon climate influenced by the Southeast Asian Monsoon circulation (Nguyen et al., 2013; UNEP, 2009). As Vietnam extends across 15 degrees of latitude from 8.30° north to 23.22° north, climatology varies significantly between the North, Central and the South parts of the country. There are seven climate zones: Northwest (B-I), Northeast (B-II), Northern Delta (B-III), North Central Coast (B-IV), South Central Coast (N-I), Central Highlands (N-II) and Southern Delta (N-III) (Fig. 1). The Vietnamese territory covers a mainland of about 332,000 square kilometers and a large area of water. The complexity of topography is shown in the digital elevation model in Fig. 2. Vietnam's geographical features together with the complex topography make the spatial distribution of climate patterns even more diverse.

2.2. Data

As rainfall and temperature are the most important elements of climate, we focus on these two variables in the analysis. The 250 land-

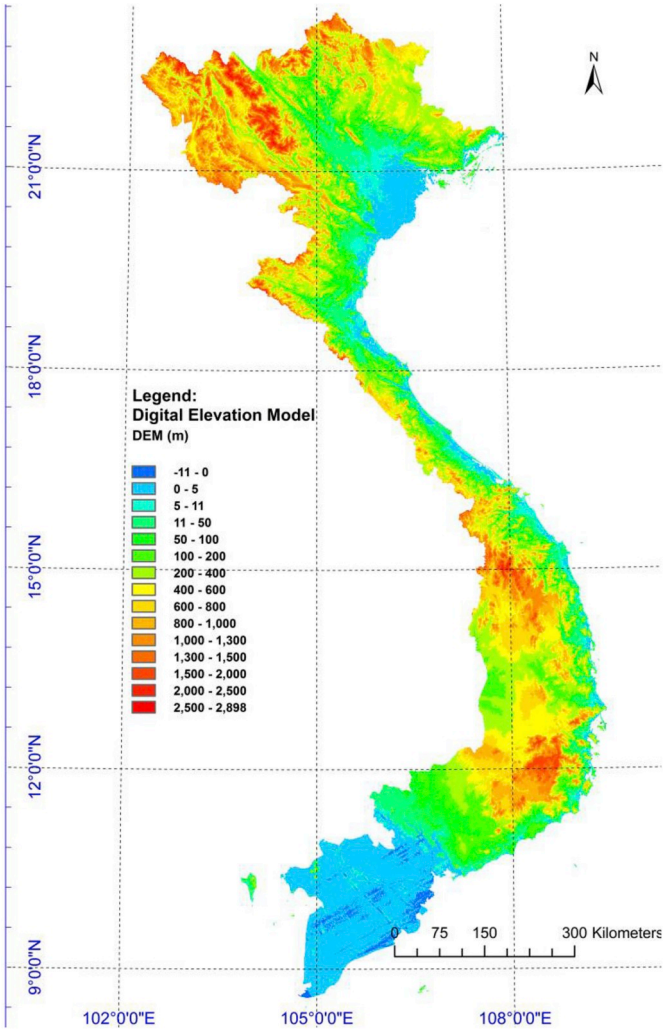

Fig. 2. Digital elevation model (DEM) of Vietnam.
Source: The digital elevation model of Vietnam was extracted from the United States Geological Survey digital elevation model raster database.

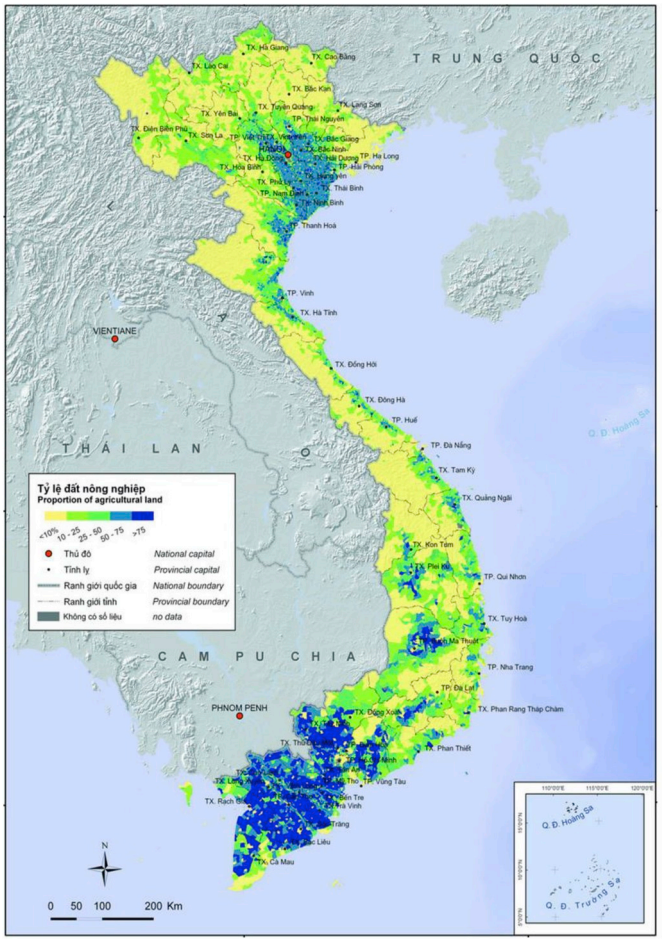

Fig. 3. Proportion of agricultural land in Vietnam.
Source: Vietnam Statistics Office (GSO)

based weather stations that report to the Vietnam National Center for Hydro-meteorological Forecasting were evaluated for data availability, timeframe consistency, and the spatial distribution in order to best represent climatic patterns and to minimize the impacts of missing data. Records of observed meteorological data were discontinuous in some regions due to the war in the 1970's. Therefore, stations where missing values exceeded 5% of total observations were excluded from the analysis as suggested by Río et al. (2011). The timeframe 1975 to 2014 was chosen for further investigation, and records of 112 out of 250 land-based weather stations widely distributed across different climatic regions of Vietnam were used in the analysis (Fig. 1). The locational coordinates of the weather stations in the study are shown in Appendix C, presented in approximate order from north to south. Due to the higher weather station network density, our dataset delivers better spatial coverage than previous studies such as Nguyen et al. (2007); Nguyen et al. (2013); Thomas et al. (2010), and consequently, substantially improves the accuracy of the interpolation techniques for climatic variables (Jones et al., 2009; Sayemuzzaman, 2014).

Maps of agricultural land use and cultivated area of rice obtained from the Vietnam General Statistics Office are used to determine the likely effects of climate change on agricultural production in the study area (Figs. 3 and 4). Based on data collected from the Rural, Agriculture and Fisheries Census, these maps show the spatial distribution of agricultural land at the commune level across the country.[1] Agricultural land is defined as the land area that is used for annual crops (e.g. rice and maize), perennial crops (e.g. rubber and coffee), and pasture grassland.

The Red River Delta in the North and the Mekong River Delta in the South have the highest proportion of land used for agricultural production (Fig. 3). A relatively high percentage of agricultural land is also identified in many communes along the coast, whereas the mountainous areas of the Northwest and Northeast, and in the Central Highlands have the lowest percentage of land used for agriculture (Fig. 3). Fig. 4 shows the distribution of the cultivated area of rice in Vietnam over the period 2005–2014. In the agricultural sector, crop production is dominated by rice as a major annual crop with an average total planted area of 7.8 million hectares per year over that period, including double or triple cropping resulting in larger annual planted areas of rice in comparison with total land area in several provinces such as Kien Giang, An Giang and Dong Thap in the South (Fig. 4). The Red River Delta in the North and the Mekong River Delta in the South have the largest planted area of rice, accounting for 15.2% and 52.8% of plantings for the whole country, respectively (Fig. 4). Some provinces such as Kien Giang, An Giang and Dong Thap in the South and Thanh Hoa, Nghe An and Thai Binh in the North are identified as the major rice production areas of Vietnam. Agricultural production, especially rice cultivation, is inherently vulnerable to climate change and variability across all regions in Vietnam. By comparing the spatial

[1] Vietnam's administration system is organized at four levels, including central, provincial, district and commune.

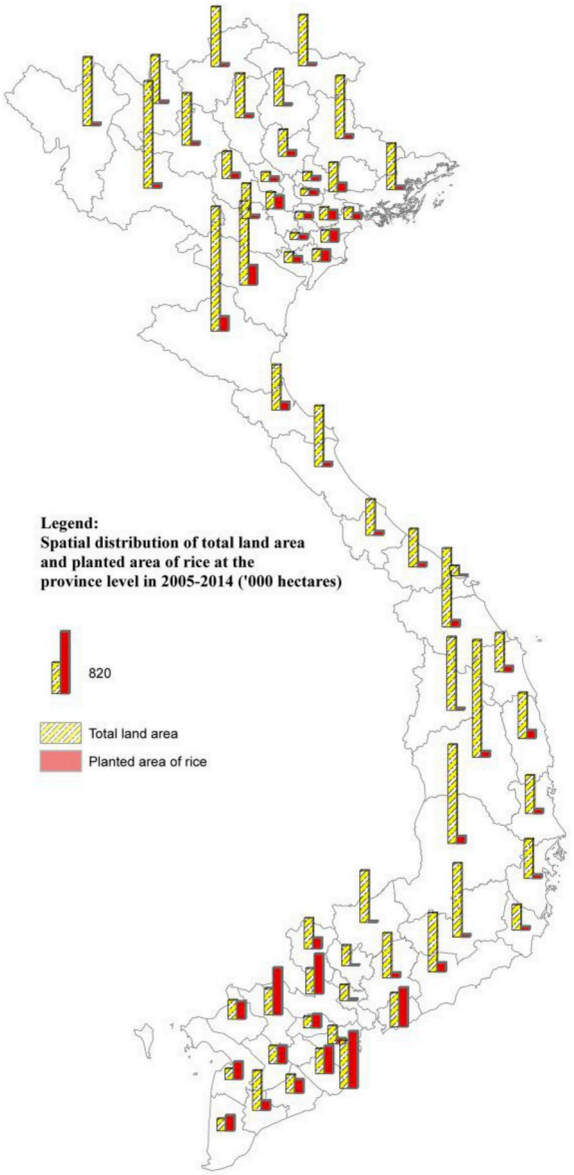
Legend:
Spatial distribution of total land area and planted area of rice at the province level in 2005-2014 ('000 hectares)
820
Total land area
Planted area of rice

Fig. 4. The spatial distribution of total land area and planted area of rice over ten years (2005–2014) at the province-level.
Source: Authors' calculation based on data from GSO, 2014

distribution of land use and climate patterns over time, it is possible to identify the potential effects of changing climatic conditions on agricultural production in Vietnam with a special focus on rice.

3. Methodology

3.1. Workflow

We applied a three-stage workflow procedure: data collection (discussed above) and organization, data homogenization, and data analysis (see Appendix D). In Step 1, to permit statistical testing for the evidence of climate change, the dataset was separated into two different periods: 1975–2004 for 30-year averages representing climate normals, and 2005–2014 to indicate current climate.

Testing for homogeneity of meteorological time series is a fundamental prerequisite for climate change studies in order to distinguish data series that are affected by non-climate factors such as changes in instrumentation and observation practices, and station relocation (Alexandersson and Moberg, 1997; Guttman, 1998; Longobardi and Villani, 2010). In Step 2, we applied several tests for homogeneity of the data that are widely used in the literature.

In Step 3, statistical testing was combined with geostatistical techniques to test the significance of trends in climatic variables, to examine the changes in temperature and precipitation patterns, and to identify the effect of those trends on rice cultivation. After confirming the presence of long-run trends in the climatic variables of interest (Pohlert et al., 2016) using the Mann-Kendall test, the co-kriging interpolation technique in ArcGIS was used to produce smoothed surface maps of precipitation and temperature patterns and to display variations across space and time.[2]

3.2. Data organization

In preparation for testing for evidence of climate change, the dataset was separated into two different periods: 1975–2004 for 30-year averages representing climate normals, and 2005–2014 to indicate current climate. According to the World Meteorological Organization, climate normals are typically defined as the three-decade averages of meteorological parameters including temperature and precipitation (Arguez and Vose, 2011). Since the values for climate normals reflect the long-term meteorological conditions or climatology, they are used to compare a current value of a meteorological variable (e.g. temperature or precipitation) to the corresponding reference value (i.e. climate normal value). Those comparisons allow identification and significance testing of changes in the climatic conditions, of long-term trends over time, and of shifts in spatial patterns of climatic variables of interest.

3.3. Data homogenization

Homogenous data time-series for climatic variables representing long-term meteorological conditions or climatology are required in climate-related studies (Buishand, 1982). Numerous methods for testing for homogeneity are found in the literature (e.g. Pettitt's test, standard normal homogeneity test, Buishand's test and Von Neumann's test), but combining several methods has proved to be more efficient because each test has particular advantages in detecting any possible break or change point within the data series (Wijngaard et al., 2003). For instance, Pettitt's test and Buishand's test are more suitable for detecting break points in the middle of the data series, while the standard normal homogeneity test is more sensitive to any change point at the beginning or the end of that series (Hawkins, 1977; Wijngaard et al., 2003). Therefore, four tests were applied to better identify non-homogeneities, with the null hypothesis of no break or change point in the data series. Calculation formulas for these tests are given in Appendix A and their advantages and limitations are in Appendix B.

These four tests for homogeneity could lead to different conclusions for an individual data series due to the differences in their power of detecting breakpoints at various locations. It is therefore necessary to generalize those conclusions to determine whether or not a particular data series is homogenous. Following Wijngaard et al. (2003), the data series were classified into different classes according to their test results for the null hypothesis of no break or shift within that series. The outcomes of the four tests were grouped into three categories:

Class A: 'useful' data series, if only one or none of the four tests rejects the null hypothesis at 1% significance level.
Class B: 'likely' data series, if two tests reject the null hypothesis at 1% significance level.
Class C: 'suspect' data series if three or four tests reject the null hypothesis at 1% significance level.

[2] Co-kriging is an interpolation technique that uses information on several variables to produce better interpolation maps. This method is discussed in detail in the next section.

Series classified in *Class C* were deemed non-homogenous time series and were not included in the next step due to the high probability of a change point within these series. Thus, data series in Classes A and B were used in the subsequent steps for trend detection. The homogeneity tests and the classification of series were applied separately for temperature and precipitation data series and the results are reported in the following section.

3.4. Statistical analysis

To integrate statistical and GIS techniques, a statistical trend test was applied to climatological variables to confirm the significance of long-term trends. Long-term upward or downward trends in observed climatic variables were assessed using the non-parametric Mann-Kendall trend test (Kendall, 1962; Mann, 1945). The test is widely applied in the literature to statistically detect a long-term trend in meteorological time series (Viola et al., 2014; Zarenistanak et al., 2014). It is a non-parametric and rank-based test, so no assumptions are required for the underlying distributional properties (Kendall, 1962; Mann, 1945; Meshram et al., 2016). The test is based on a calculation of the Kendall's Tau S statistic value under the null hypothesis of no trend existing in the series of records.

Suppose that there exists a pair of observed values x_i, x_j $(i > j)$ in a series of a meteorological variable of a sequence $x_1, x_2 \ldots x_n$ with n observations. An S statistic value is calculated based on pairwise comparisons of each observed value j with all preceding observed data points i as:

$$S = \sum_{i=1}^{n-1} \sum_{j=i+1}^{n} sign(x_j - x_i), \tag{1}$$

where

$$sign(x_j - x_i) = \begin{cases} 1, if\ (x_j - x_i) > 0 \\ 0, if\ (x_j - x_i) = 0 \\ -1, if\ (x_j - x_i) < 0 \end{cases} \tag{2}$$

Kendall (1962) postulates that S is approximately normally distributed with expected value $E(S) = 0$ and variance Var(S):

$$Var(S) = \frac{1}{n}\left[n(n-1)(2n+5) - \sum_t t(t-1)(2t+5)\right], \tag{3}$$

where t is a time index. The standardized Z value could be calculated as follows:

$$Z = \begin{bmatrix} -1, & if\ S < 0 \\ \frac{S+1}{\sqrt{Var(S)}}, & if\ S > 0 \\ 0, & if\ S = 0 \end{bmatrix} \tag{4}$$

The test is performed by comparing the absolute value of Z to the critical value of a standard normal distribution to identify the significance level of the trend.

3.5. Visual analysis using geostatistical approach

Geostatistical techniques have benefitted enormously from the development of Geographical Information Systems (GIS). In graphical representations of climate data, more user-friendly applications have been used widely by practitioners to accurately and efficiently model spatio-temporal patterns of climatic variables of interest (Johnston et al., 2001; Moral, 2010). As climate data are only observed at certain places, there is a need to predict this information for other locations. Consequently, there is an increasing demand for interpolated surfaces of climate variables using weather station-level data with a wide range of geostatistical methods applied such as inverse distance weighting, kriging or co-kriging, and kernel smoothing. Among those, co-kriging has certain advantages because it takes into account cross-correlations between covariates (such as temperature and elevation) to make better interpolation predictions (Cressie, 2015; Moral, 2010; Ninyerola et al., 2000; Pardo-Igúzquiza, 1998; Prudhomme and Reed, 1999).

In climate mapping, there is often a strong relationship between elevation and climatic variables such as temperature and precipitation: precipitation generally increases with elevation whereas temperature often decreases as elevation increases (Daly et al., 2008). Due to the complexity of topography across weather stations in our study areas, there may be correlation between meteorological variables and elevation at the same location. The co-kriging interpolation technique is used to map the spatial distribution of rainfall and temperature in connection with topographical features extracted from the digital elevation model.

The theoretical basis and mathematical formulas of co-kriging are discussed by Cressie (2015), Moral (2010) and Pardo-Igúzquiza (1998). This method predicts the unknown value of a primary variable of interest at a given location using information on the measured values of the primary variable and of an auxiliary variable. The auxiliary variable, such as elevation, is expected to be correlated with the primary variable, e.g. temperature, so that it can provide additional information that will help achieve more accurate estimate. The co-kriging technique takes into account the correlation between the primary and auxiliary variables and also the spatial correlation across observed values at various locations.

The Geostatistical Analyst extension of the ArcGIS 10.4 software was applied to produce interpolated surfaces using the ordinary co-kriging method for the variables of interest. Subsequently, a set of interpolated map layers of rainfall and temperature for two periods (climate normals for 1975–2004 and the current climate for 2005–2014) was generated for further analysis.

Two variables were considered in this case: Z_1 as a primary climatic variable and Z_2 which is derived from the digital elevation model as an auxiliary covariate of elevation at a given location (s). The ordinary co-kriging can be represented by the following models (Johnston et al., 2001; Journel and Huijbregts, 1978)[3]:

$$\begin{aligned} Z_{1(s)} &= \mu_1 + \varepsilon_{1(s)} \\ Z_{2(s)} &= \mu_2 + \varepsilon_{2(s)}, \end{aligned} \tag{5}$$

where μ_1 and μ_2 are unknown constants; $\varepsilon_{1(s)}$ and $\varepsilon_{2(s)}$ are error terms with possible cross-correlation and autocorrelation.

Our goal is to predict the unknown value of the primary climatic variable at location s_0, denoted $Z_{1(s0)}$, based not only on the value for that variable recorded at the nearest weather station (Z_1), but also on the information on the auxiliary elevation covariate (Z_2) because of the strong correlation between the two. Thus, the primary climatic variable, the autocorrelation for each variable, and the cross-correlation between variables are used to produce robust predictions of $Z_{1(s0)}$. The co-kriging predicted value $\hat{Z}_1(s_0)$ is a linear combination of all available data points of the two variables of interest (primary and auxiliary):

$$\hat{Z}_{1(s_0)} = \sum_{i=1}^{n} \lambda_{1i} Z_{1i} + \sum_{i=1}^{n} \delta_{2i} Z_{2i}, \tag{6}$$

where λ and δ determined by the co-kriging tool are the spatial weights across data points in the sample.

To obtain an unbiased predictor, the deviations between the predicted values and the observed points were minimized (Cressie, 2015):

$$E\left[\hat{Z}_{1(s_0)} - \left(\sum_{i=1}^{n} \lambda_{1i} Z_{1i} + \sum_{i=1}^{n} \delta_{2i} Z_{2i}\right)\right]^2 \tag{7}$$

After interpolating, a set of smoothed surface maps of each climatic variable for climate normals and current climate were created. Given

[3] Additional explanations of the co-kriging technique are in Cressie (2015), Johnston et al. (2001) and Journel and Huijbregts (1978).

Table 1
Summary results of homogeneity tests for meteorological data series.

Precipitation series				Temperature series			
Classes	Homogeneity	Number of stations	%	Classes	Homogeneity	Number of stations	%
A	Yes	78	69.6	A	Yes	43	38.5
B	Likely	21	18.8	B	Likely	32	28.5
C	No	13	11.6	C	No	37	33.0
Total		112	100	Total		112	100

the seasonality of precipitation and temperature, there is a need for a standardized process that is able to capture and display monthly predicted values in the interpolated maps. This helps better visualize the interpolation outcomes and makes these graphics visually comparable across space and time.

To address this, certain common criteria were set up for the output rasters, for example, projected coordinate systems (WGS_1984_UTM_Zone_48N), cell size ($0.008333 \times 0.008333 \sim 1\ km^2$), pixel type (signed 16 bit), and color ramps.[4] More specifically, to create a color ramp, a unique color was manually assigned for an individual group of predicted values, so that the ramp can cover all possible ranges of values of rainfall or temperature in different time periods (months). The final interpolated maps are produced using a mosaic dataset technique which contains our specified function chains (e.g. colormap, hillshade function, clip function …) to efficiently display the interpolated surface in connection with the site-specific topographical features.[5]

In geoprocessing raw data for co-kriging and publishing outputs, our workflow contains a number of repeated steps applied at each time-step within the time series of the meteorological variables. Model Builder tool within ArcGIS provides the interactive means to accurately and efficiently reproduce these geoprocessing procedures. A base model was first constructed using Model Builder tool that was applied to a specific task, such as interpolating annual mean temperature. Then, all necessary modifications were made to the model (such as input and output sources and function parameters) to re-apply that process to another variable. This automated workflow allowed us to avoid mistakes that are likely to be associated with other geoprocessing procedure (Pil, 2013).

4. Results and discussion

4.1. Homogeneity tests

The results of homogeneity analysis for meteorological data series are presented in Table 1 based on the outcomes of Pettitt's test, standard normal homogeneity test, Buishand's test, and Von Neumann's test. These tests determine whether or not the observed time series at each station is homogenous at the 1% significance level. As discussed in Section 3.3, the data series were classified into three different classes based on the results of the four homogeneity tests. For precipitation, the majority of data series are *Class A* and *Class B*, i.e. homogenous, whereas 11.6% of the 112 stations fall in the non-homogenous *Class C*. In contrast, the series for temperature show a relatively large number of stations (33% of the 112 stations) characterized by non-homogeneity. Non-homogenous data series of either precipitation or temperature (*Class C*) that make these variables unrepresentative of temporal climate variability and change are excluded from the geophysical data visualization and statistical trend tests in the next step.

4.2. Statistical analysis of trends

It is important to test whether observed climate variations represent long-term trends over time and space or are just short-term movements in climatic conditions. Long-term upward or downward trends in observed climatic variables were assessed using the non-parametric Mann-Kendall trend test with a null hypothesis of no change in the data series at the 10% significance level (Kendall, 1962; Mann, 1945).

4.2.1. Trends in precipitation

Fig. 5 shows a map of trends in precipitation over the 1975–2014 period. The map presents *Z* statistic values of the Mann-Kendall test representing the sign, magnitude, and significance level of the long-term trends.

The geospatial distribution of trend test results for precipitation shows a large and significant variation across Vietnam (Fig. 5). There is statistically significant evidence that out of 99 land-based weather stations with data series confirmed homogenous by the homogeneity tests, 23 stations show an increase in rainfall over 1975 to 2014 and 19 stations show a decrease. The majority of meteorological stations (57.6%) have insignificant long-term changes in precipitation.

Considering the magnitude of the changes using the Z values of the Mann-Kendall trend test in Fig. 5, the trend of increasing precipitation is relatively pronounced in the north-westernmost regions and the center of the Central Coast (B-IV and N-I) of Vietnam. The magnitude of change in rainfall trend is moderate in the western areas of the Southern Delta (N-III). Trends of decreasing rainfall are scattered throughout the country with some noticeable rainfall-deficit areas such as parts of the Northern Delta (B-III), the northernmost regions of the North Central Coast (B-IV), the Central Highlands (N-II), and the coastal side of the Southern Delta (N-III).

4.2.2. Trends in temperature

Mann-Kendall trend test results show a relatively uniform distribution of temperature patterns across regions (Fig. 5). In most parts of the country, a statistically significant warming trend dominates. Over half (58.6%) of the meteorological stations show a statistically significant long-term increase in temperature, while only 14.2% of stations have a decreasing temperature, and 26.6% of stations have no significant change (Fig. 5). All stations that have recorded decreasing temperature trend are located in the northern parts of the Central Coast and the North of the country. The greatest increasing temperature trend is identified in the center of the North part of the country (B-III), the northernmost and southernmost regions of the Central Coast (B-IV and N-I), and parts of the Central Highlands (N-II) and the Southern Delta (N-III).

4.3. Geostatistical analysis

For the purpose of visual analysis, procedures described in Section 3 were applied using the Geostatistical Analyst extension in ArcGIS combined with a mosaic dataset technique to produce and export the

[4] Before creating an output for a raster dataset, the pixel type specifies the bit depth of that output. Here, the bit depth of signed 16 bit can contain a range of values between −32768 and 32767 in each pixel. A color ramp provides a means to apply a range of specified colors to the corresponding range of values from the interpolated surface.

[5] A mosaic dataset can be used to combine multiple individual rasters and then display them in an exported map at once using specified function chains.

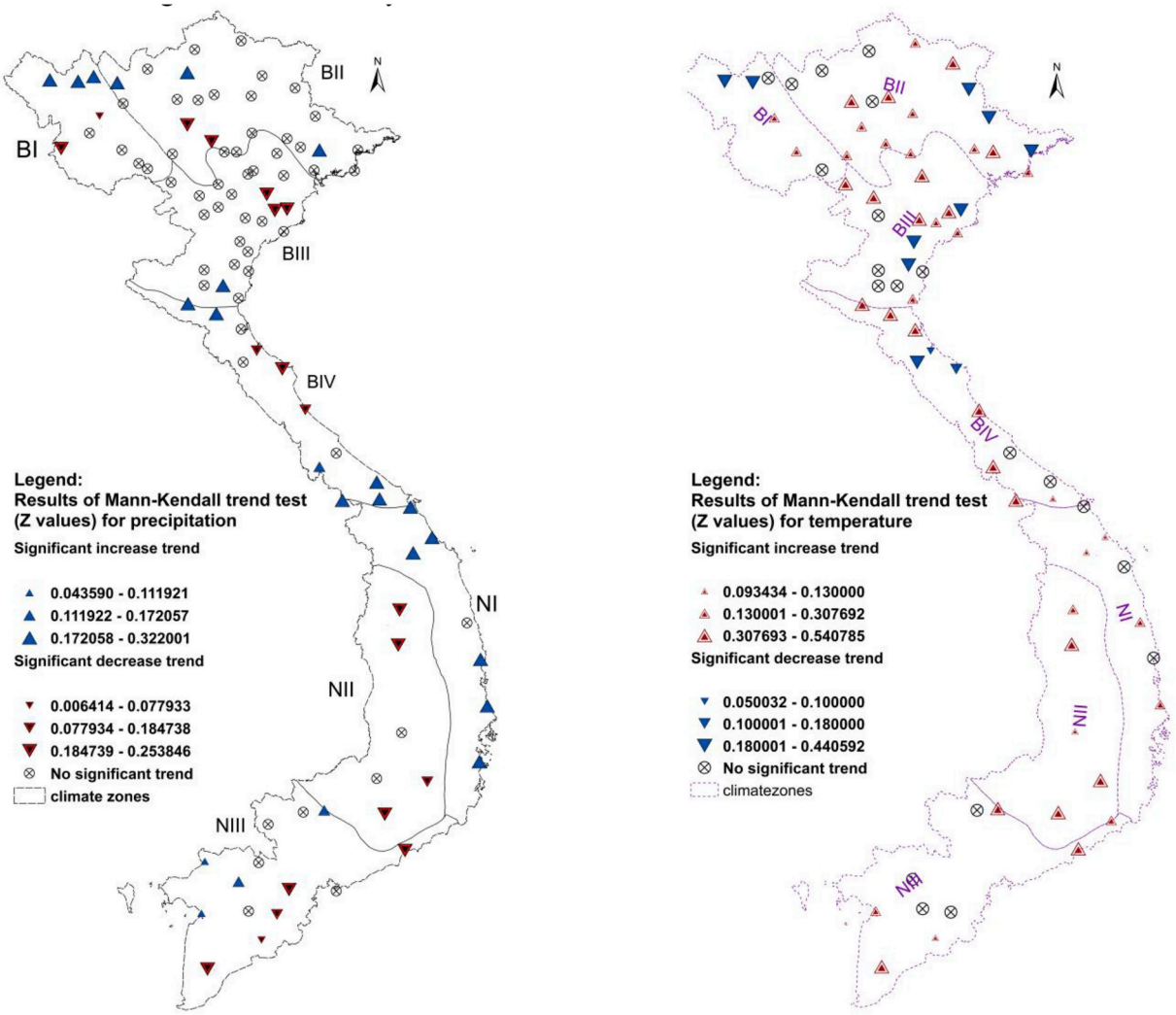

Fig. 5. Results of Mann-Kendall trend test for precipitation (*left*) and temperature (*right*).

smoothed interpolated surfaces of rainfall and temperature. The outcomes are displayed as three consecutive digital maps of climate normals, current climate, and climate anomalies – defined as the deviation of the current climate from the normal climate (Figs. 7 and 8).

4.3.1. Observed precipitation patterns

4.3.1.1. Analysis of mean annual precipitation changes. The spatial distribution of average annual rainfall in both current and baseline periods varies considerably across regions (Fig. 6). Some areas have seen an increase in precipitation while others have experienced a decrease. Generally, locations with high elevation such as the mountainous areas in the Northwest and Central Highlands receive higher rainfall. For climate normals, the highest rainfall is in the Northwest (B-I), North Central Coast (B-IV), Central Highlands (N-II) and the southernmost area of the Southern Delta (N-III). However, recent climatic conditions (2005–2014) have been changing remarkably with a pronounced drying pattern observed in many regions, such as the Northern Delta (B-III) and the South Central Coast (N-I) (Fig. 6-b).

The map of rainfall anomalies on the right in Fig. 6 demonstrates a dramatic heterogeneity in the distribution of precipitation change across regions. Rainfall deficit seems to be spreading throughout the country with a number of 'hotspots' like the westernmost provinces in the Northwest (B-I), the Red River Delta (B-III), the North Central Coast (B-IV), the northernmost of the Central Highlands (N-II), parts of the Mekong River Delta, and parts of the coastal regions in the South. In contrast, the north-western area of the country shows a significant rainfall increase. Annual rainfall has also been increasing considerably in Thua Thien Hue and Quang Nam provinces in the middle of the Central Coast (Fig. 6-c).

In the areas where we identified a marked decline in precipitation, there is a very high proportion of land used for agricultural production, and particularly for rice cultivation. The two largest deltas of the Red River and the Mekong River account for 68.7% of the total 7.8 million hectares of the rice cultivated in Vietnam (Figs. 3 and 4). More importantly, significant changes in the pattern of rainfall are observed in provinces with substantial areas of rice (Fig. 4): Kien Giang (753,600 ha), An Giang (625,800 ha) and Ca Mau (127,400 ha) in the Mekong area, and Thanh Hoa (258,600 ha) and Thai Binh (161,800 ha) in the lowland areas of the North. These rainfall pattern changes in provinces with large rice cultivation areas are likely to affect rice production. There is a strong evidence of the influence of changes in

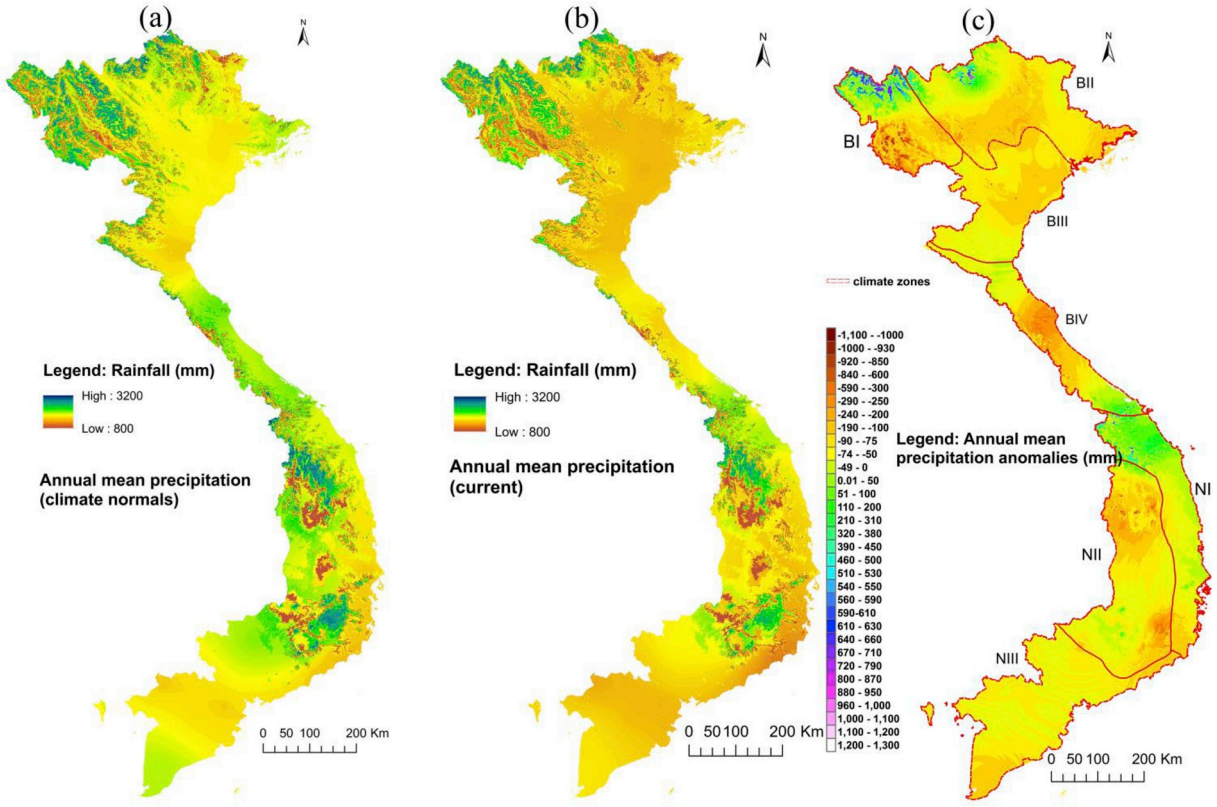

Fig. 6. Spatial distribution of mean annual rainfall for climate normals *(a)*, current climate *(b)*, and climate anomalies *(c)*.

rainfall patterns on crop yields, particularly yield reduction due to water scarcity in crops like rice (Nelson et al., 2009). Also, altered rainfall patterns are likely to be associated with increasing intensity of extreme weather events, and pests and plant diseases in rice-growing areas (Rosenzweig et al., 2001).

Overall, visualizing the spatio-temporal distribution of precipitation allows effective displaying and highlighting the rainfall pattern changes and identifying their potential impacts on agricultural production. Since climate-related variables are associated with seasonality, these variables were further explored at monthly intervals to gain greater insight into the underlying distributions of climate processes.

4.3.1.2. Analysis of total monthly precipitation changes. The changes in the monthly precipitation patterns from region to region and over time are shown in Fig. 7. The maps show that monthly variations of rainfall in Vietnam are strongly pronounced. For the first four months from January to April (Fig. 7.1), the rainfall is relatively low and unevenly distributed all over the country. Slightly more rain has been recorded recently in March and April compared to the baseline of the 30-year average from 1975 to 2004.

However, in the four months of the summer season, there was a remarkable change in precipitation amount and its pattern (Fig. 7.2). Rainfall from May to August shows very high rain totals in the Northwest (B-I), the Central Highlands (N-II), and the southernmost regions of the Southern Delta (N-III). Compared to climate normals, current climatic conditions during May to August clearly demonstrate different trends, including a substantial increase in total rainfall in the northwest of the country versus a significant decrease in total rainfall in the Central Highlands (N-II) and in the rest of the north-western area.

From September to December (Fig. 7.3), the rainfall patterns move southward with higher precipitation observed in the Central Coast (B-IV and N-I), the Central Highlands (N-II), and the Southern Delta (N-III), while the northern regions of the country are dominated by drier conditions. In particular, the current climate of the Central Coast (B-IV and N-I) and southern areas shows a significant increase in the amount of rain in November and December. Considering climate anomalies from September onwards, there is now very strong evidence of rainfall variability and change from region to region. In Fig. 7.3, that evidence can be clearly observed and is even more pronounced compared to previous periods by the noticeable rainfall deficit in the northern Central Coast (B-IV and N-I) and, simultaneously, a strongly increasing precipitation in the center of Vietnam.

Overall, there are remarkably sharp contrasts in the monthly distribution patterns of rainfall variability and change across regions of Vietnam. The growing season for rice varies across regions and can extend from 1 February to 30 December (VAAS, 2010). In the North, the winter-spring rice season starts in early February and continues to the middle of June. Considering rainfall anomalies during this period, more precipitation has been observed in the Northwest (B-I) whereas other areas in the North exhibit notably less precipitation, especially in the month of June. This rainfall pattern change is likely to have adverse impacts on rice cultivation in this season. For the spring-autumn season (June–November), a similar trend is observed in the early season but not for the last few months of the year of September, October, and November.

In contrast, in the Central Coast, it is hard to notice any significant climatic change during the winter-spring season for rice (February–May). However, in the spring-autumn season (June–October/December), the rainfall pattern changes dramatically combining both a decrease in the northern areas and a significant

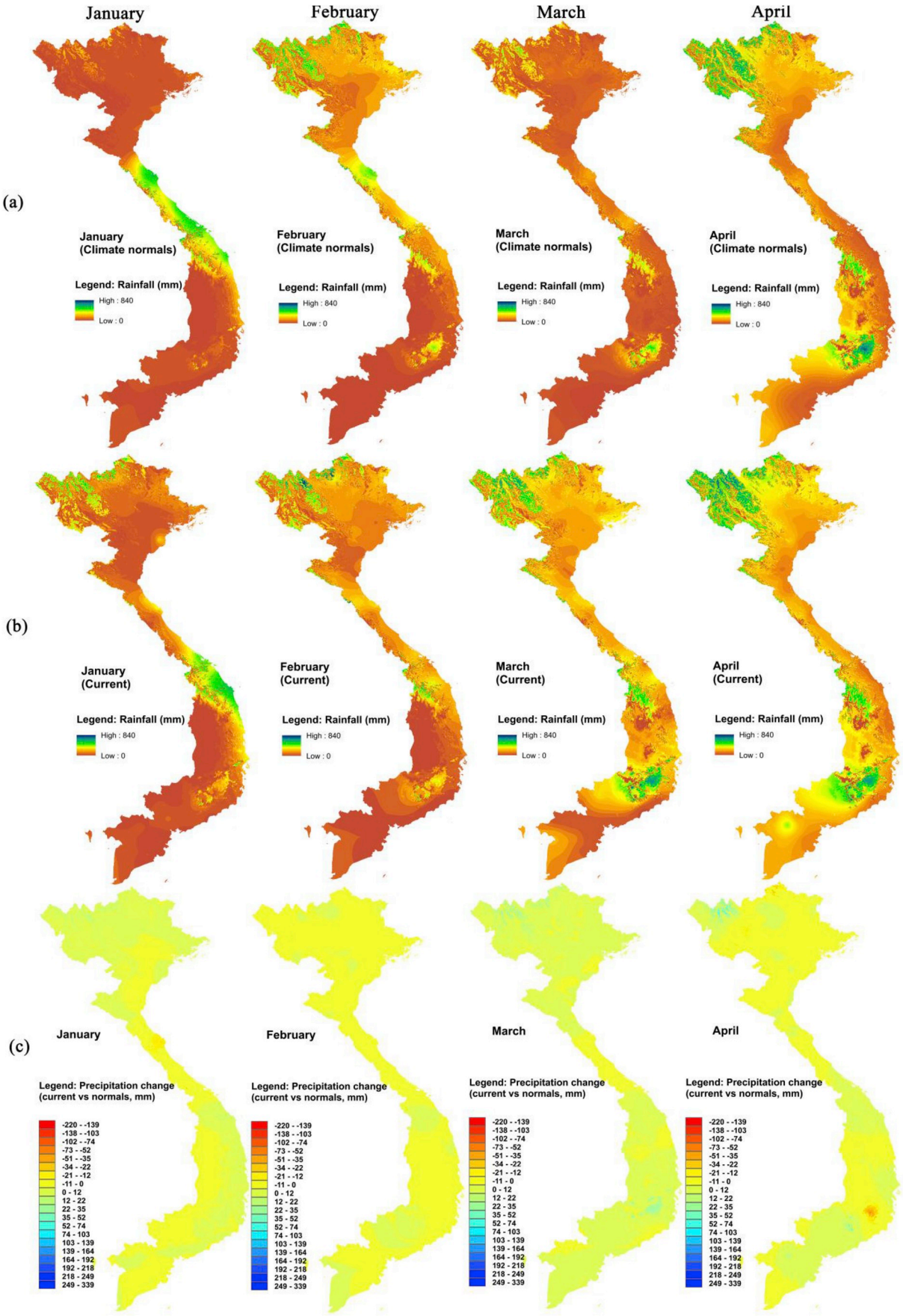

Fig. 7. 1. Spatial distribution of monthly precipitation for January to April for climate normals *(a)*, current climate *(b)*, and climate anomalies *(c)*. 2. Spatial distribution of monthly precipitation for May to August for climate normals *(a)*, current climate *(b)*, and climate anomalies *(c)*. 3. Spatial distribution of monthly precipitation for September to December for climate normals *(a)*, current climate *(b)*, and climate anomalies *(c)*.

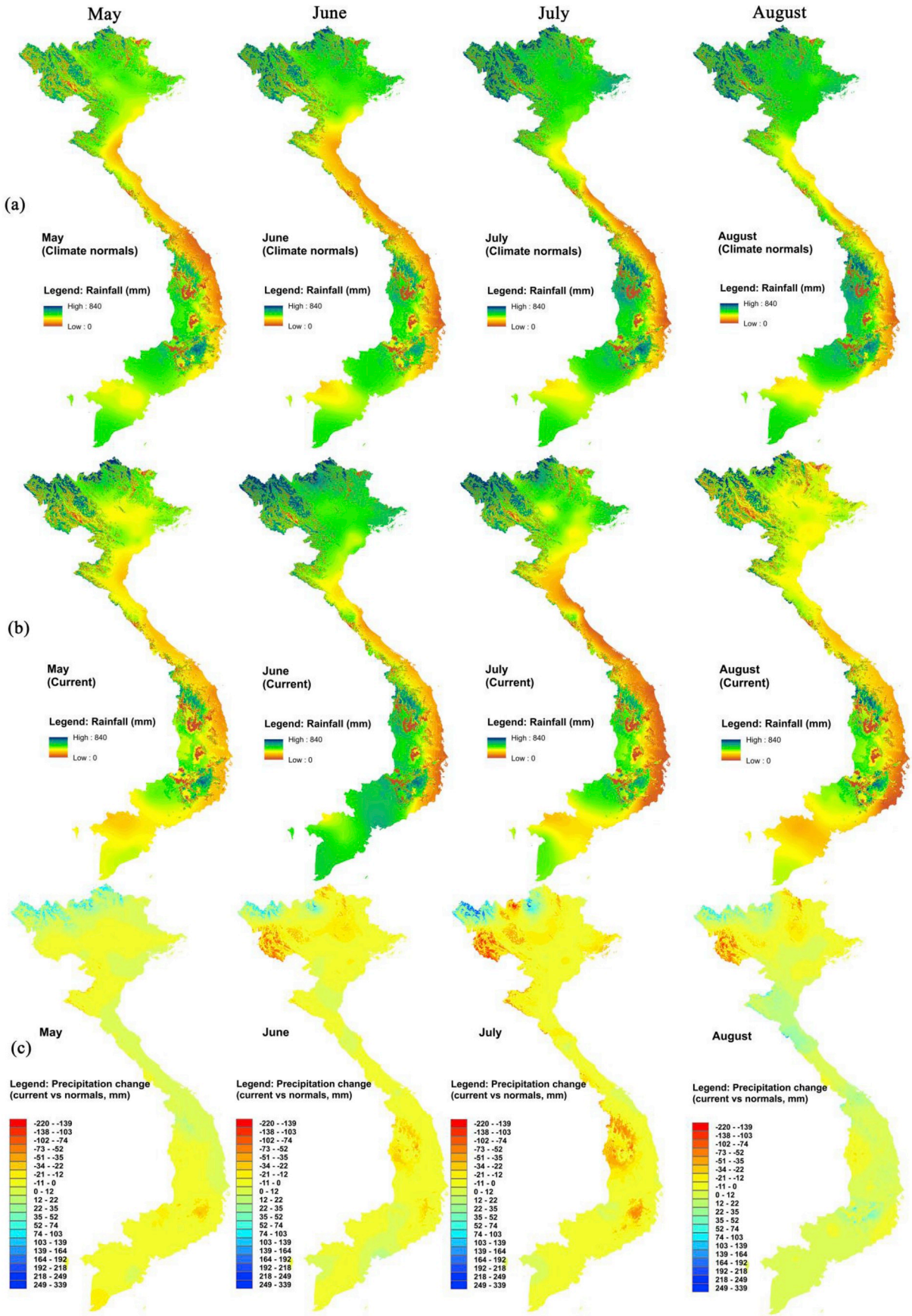

Fig. 7. (*continued*)

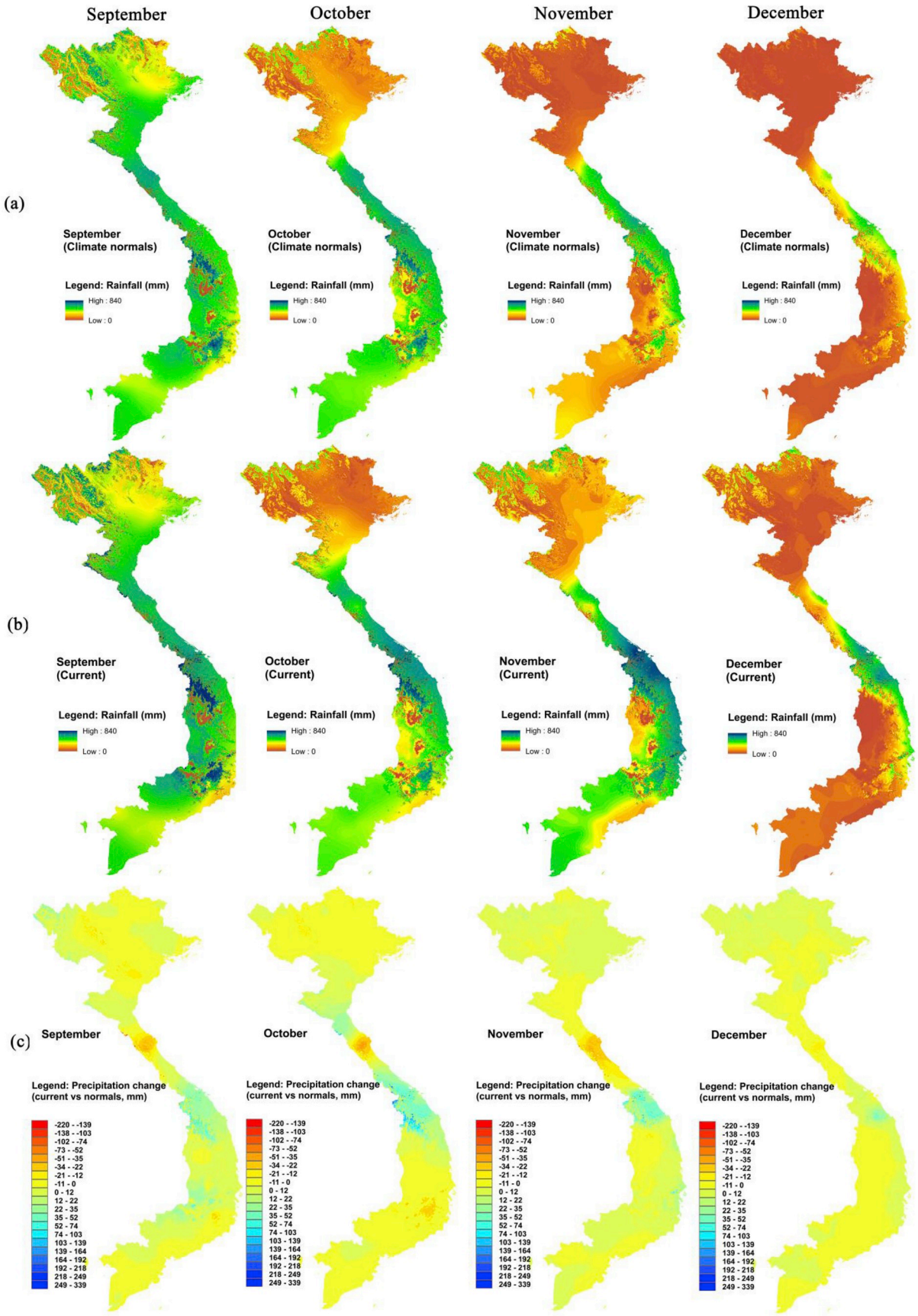

Fig. 7. (*continued*)

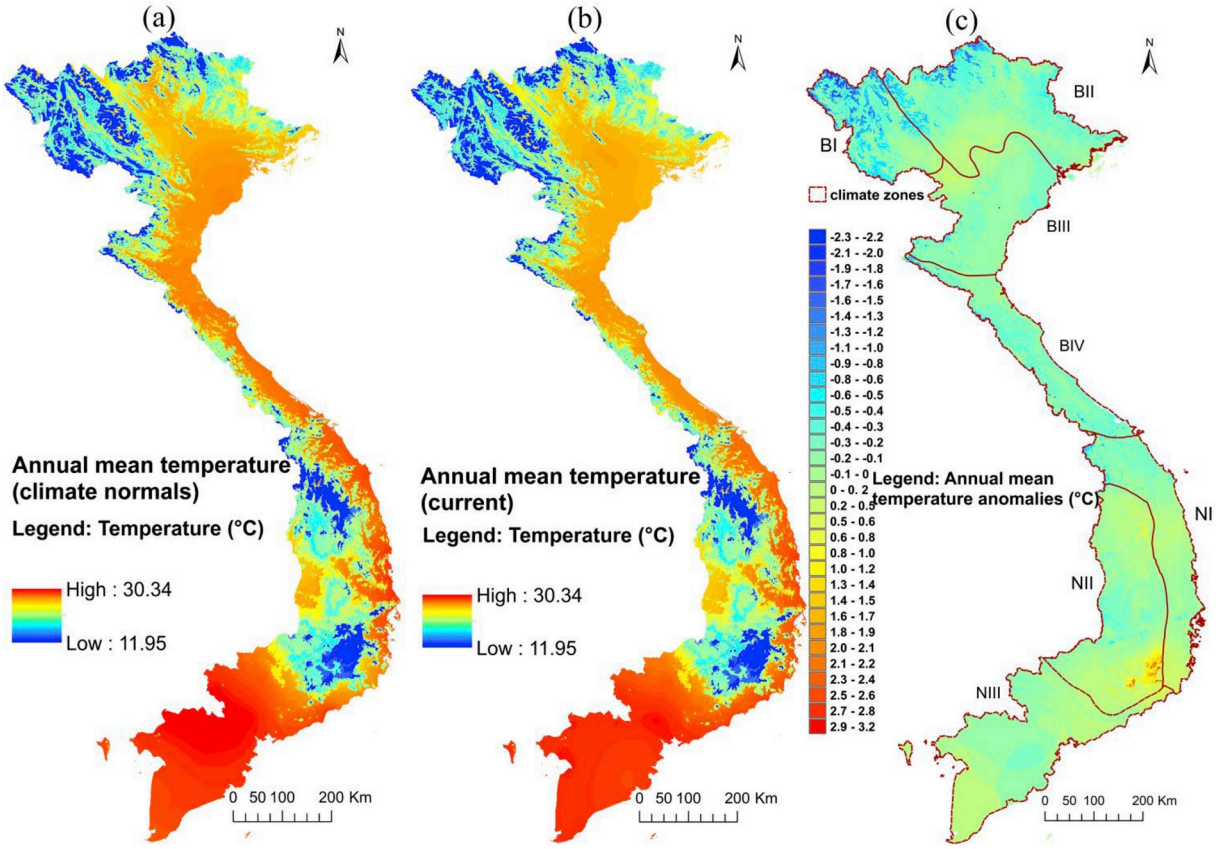

Fig. 8. Spatial distribution of mean annual temperature for climate normals *(a)*, current climate *(b)*, and climate anomalies *(c)*.

increase in many southernmost areas of the Central Coast. Those notable rainfall anomalies, either deficiency or surplus, could have large detrimental effects on rice production in those regions since the crop requires a specific amount of water at regular time intervals during the growing season. Similarly, in the South, both increases and decreases in rainfall are observed across locations, with a very high rainfall deficit in the northernmost area of this region.

4.3.2. Observed temperature patterns

4.3.2.1. Analysis of annual mean temperature. Fig. 8 shows the spatio-temporal changes of annual average temperature across regions of Vietnam. Because Vietnam extends across 15 degrees of latitude, its temperature pattern varies significantly between North, Central, and South with a noticeably higher mean temperature in the southern areas, which are closer to the equator. This spatial temperature pattern appears unchanged in the two defined periods of the climate normals (1975–2004) and the current climate (2005–2014) (Fig. 8-a and 8-b). During the two defined periods, the annual average temperature ranges between 11.95 and 30.34 °C. Lower mean temperatures are observed in the Northwest (B-I) and Central Highlands (N-II), whereas in the Southern Delta (N-III) and Central Coast (B-IV and N-I) the average temperature is typically higher.

Temporal shifts in observed temperature have been found across space when comparing the current climatic conditions with the 30-year average conditions, which is a robust signal of temperature variability and change in Vietnam (Fig. 8-c). Climate anomalies in temperature show diverse patterns, mixing both increasing and decreasing trends in various locations, where some areas may experience more warming or cooling than others. Long-term temperature increase is especially significant in the southernmost areas of the Central Highlands (N-II) with the magnitude of the anomaly as high as 3.2 °C. In contrast, temperature decrease relative to the climate normals has dominated in the regions of the Northwest (B-I), with the lowest decrease recorded of −2.3 °C (Fig. 8-c).

Overall, a pattern of increasing average temperature is observed in the rice-cultivating areas including the Red River and Mekong River deltas (Figs. 4 and 8), which is likely to be detrimental for rice cultivation due to worsening drought conditions. More specifically, some provinces with large areas of rice cultivation such as Kien Giang and Ca Mau in the Mekong Delta, Binh Thuan and Quang Ngai in the Central Coast, and Thanh Hoa, Nghe An, Thai Binh and Phu Tho in the northern areas experienced a notable increase in temperature. There is also a growing evidence that warming climate likely increases the severity of plant diseases and water shortages leading to a reduction in productivity. Consequently, it is expected that the rice sector will be hard hit by the warming pattern. Because only looking at annual mean temperature may miss the monthly changes across the year, the observed temperature series at the monthly scale are further explored below.

4.3.2.2. Analysis of monthly mean temperature. Fig. 9 shows the spatio-temporal distribution of monthly mean temperature and its variability across the country. Changes in monthly temperature have been taking place across the whole country compared to the long-term climate normals. Observations of the warming pattern are very common in many locations from the North to the South of Vietnam such as the Northern Delta (B-III), the South Central Coast (N-I), the Central Highlands (N-II), and the Southern Delta (N-III). A warming pattern is observed over most months in the year, with an exception in June with

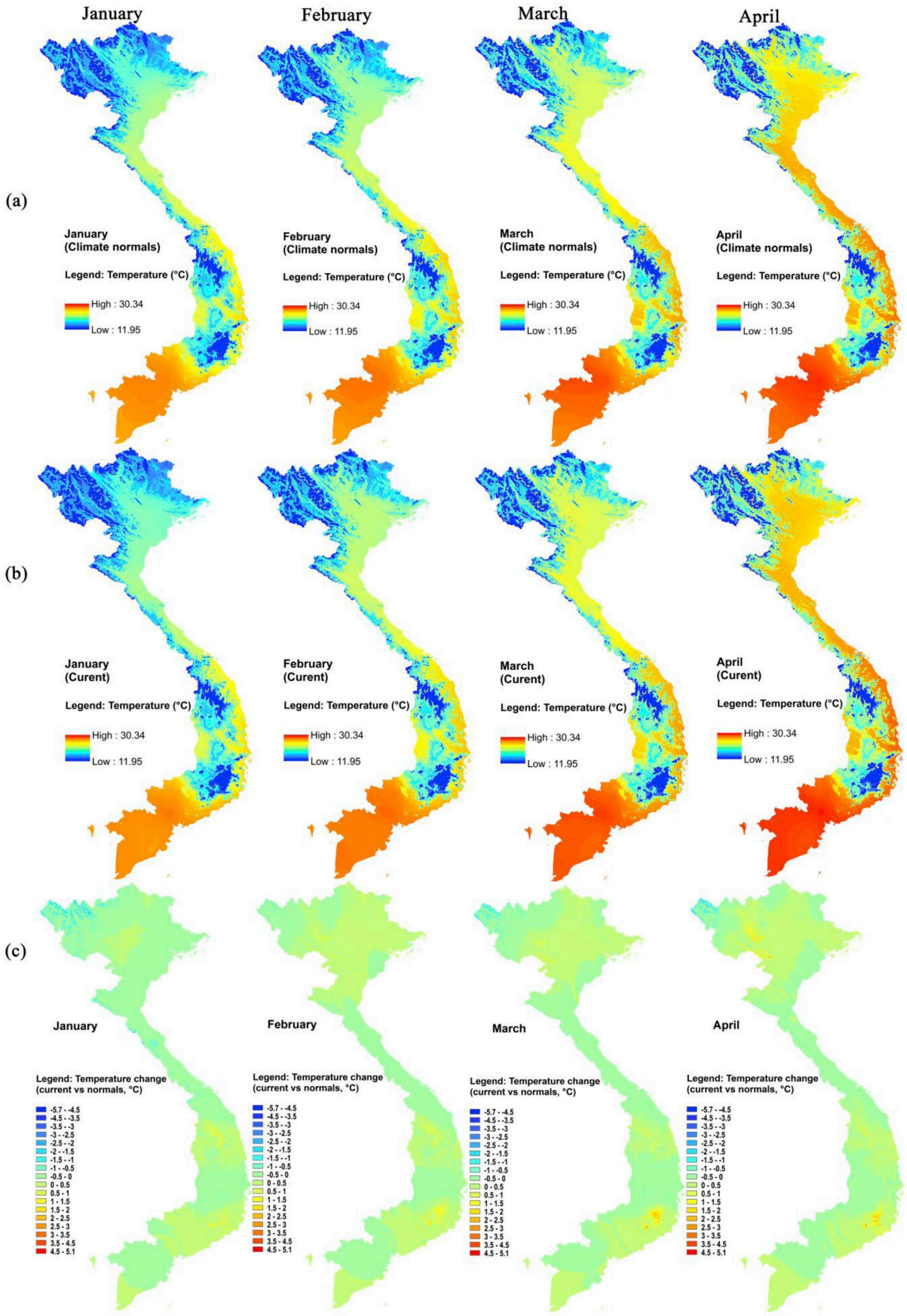

Fig. 9. 1. Spatial distribution of monthly temperature for January to April for climate normals *(a)*, current climate *(b)*, and climate anomalies *(c)*. 2. Spatial distribution of monthly temperature for May to August for climate normals *(a)*, current climate *(b)*, and climate anomalies *(c)*. 3. Spatial distribution of monthly temperature for September to December for climate normals *(a)*, current climate *(b)*, and climate anomalies *(c)*.

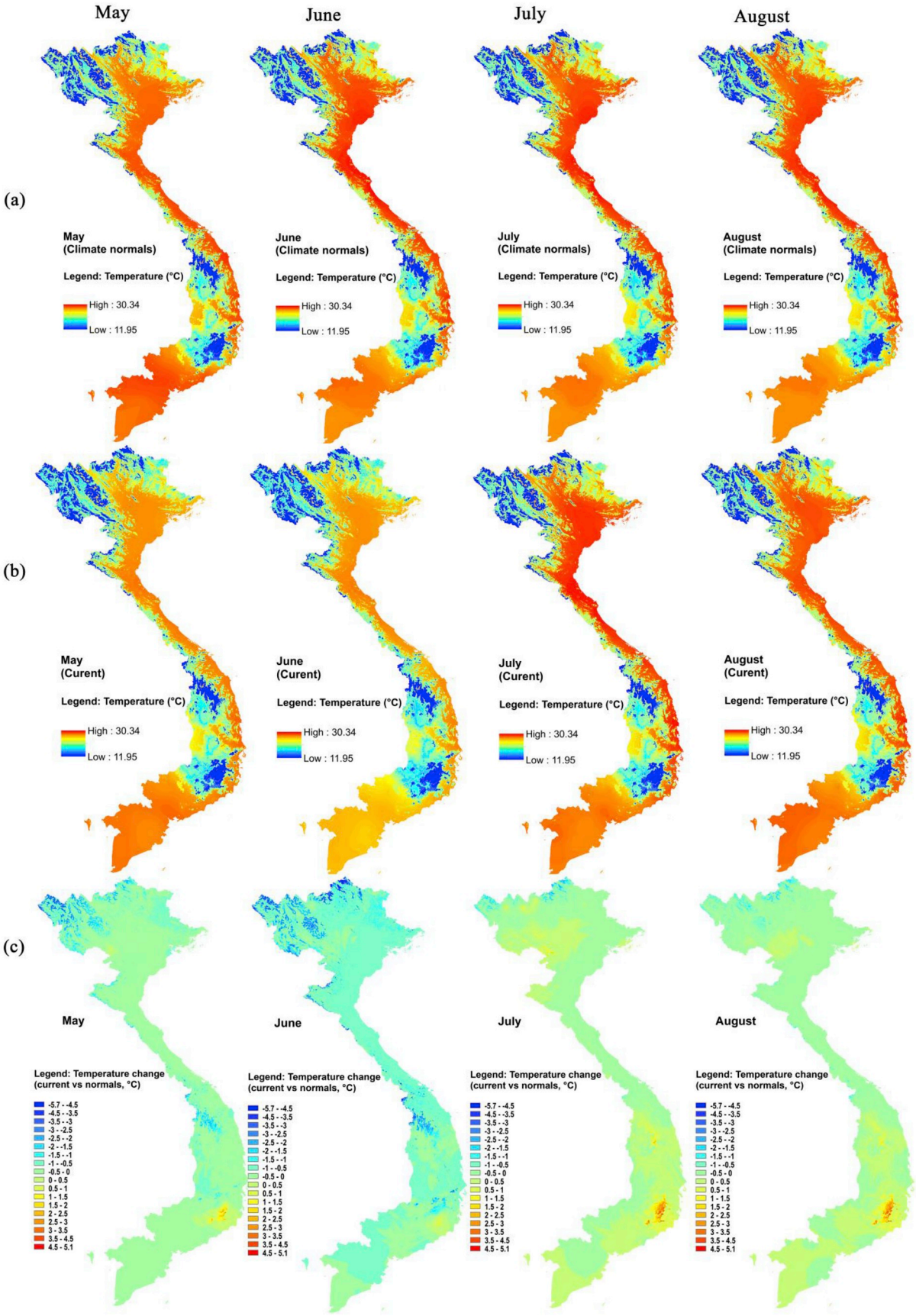

Fig. 9. (*continued*)

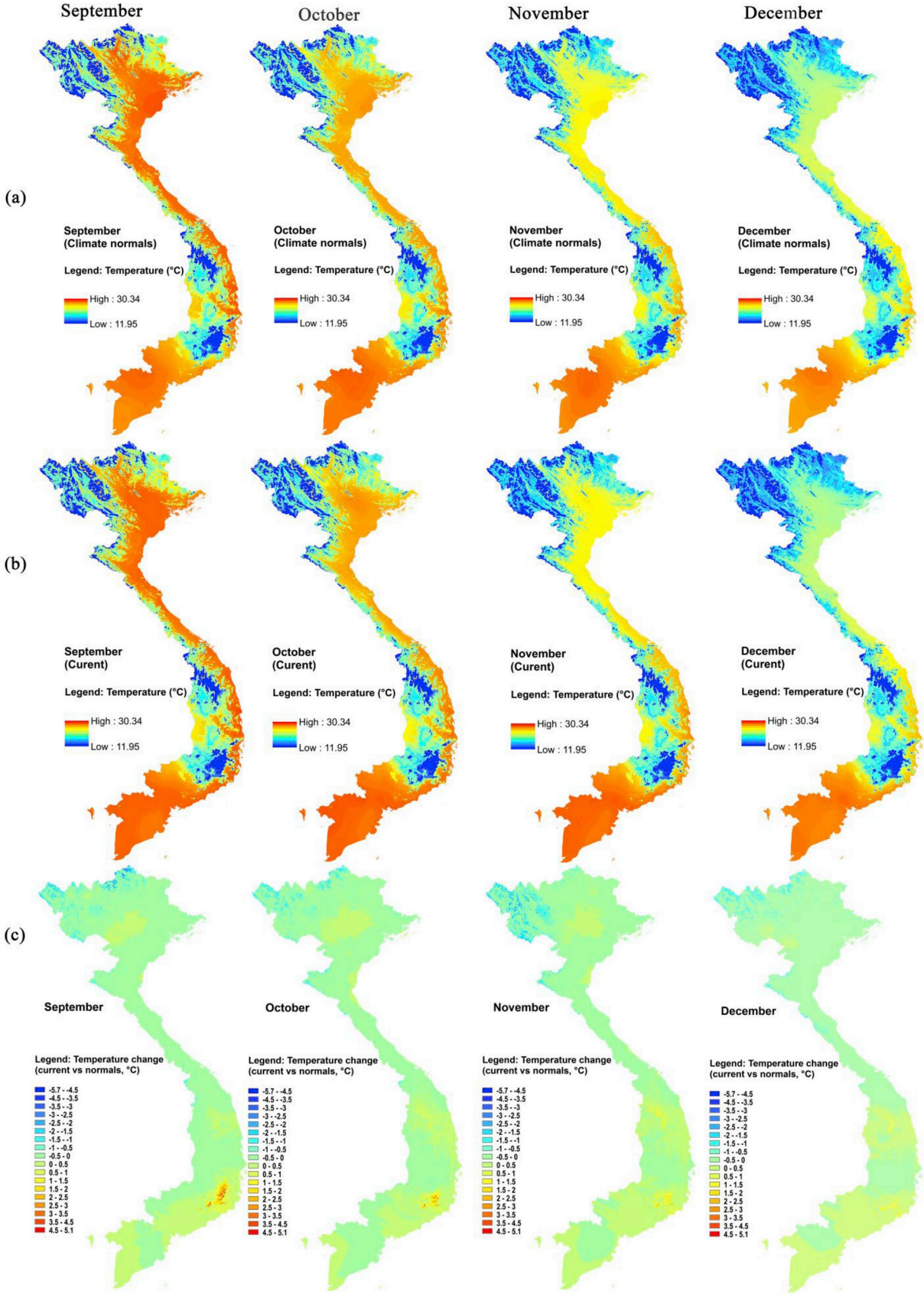

Fig. 9. (*continued*)

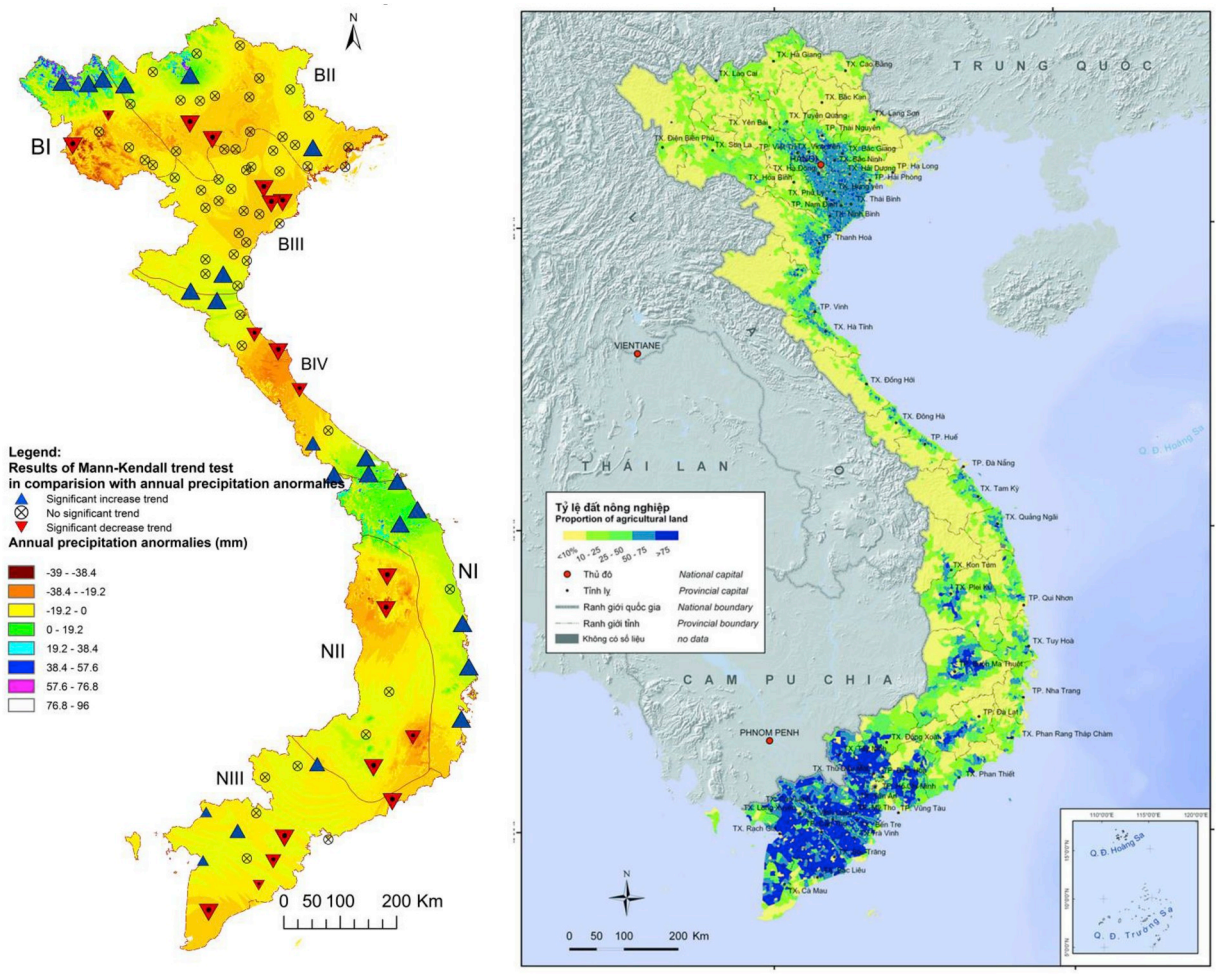

Fig. 10. Results of Mann-Kendall trend test comparing annual mean precipitation anomalies *(left)* and the distribution of agricultural land in Vietnam *(right)*.

a cooler mean temperature under current climatic conditions.

Maps of the surface temperature anomalies depict even clearer trends of widespread patterns of increasing average surface temperature across the country, especially in the center of the Northern Delta (B-III), the South Central Coast (N-I), and part of the Southern Delta (N-III). Those variations in the temperature are the most direct sign that climatic conditions are changing (USEPA, 2016). Furthermore, the highest warming rate is identified in the southernmost region of the Central Highlands and the Central Coast including Dalat, Ninh Thuan and Binh Thuan provinces. The monthly temperature in July–August in these provinces is over 5.1 °C warmer in the current climate compared to the long-run average (Fig. 9.2-c). Overall, compared with the patterns for precipitation, the spatio-temporal changes in temperature show a clear tendency characterized by a warming pattern across Vietnam. The visual analysis used in mapping the distribution of temperature contributes significantly to analyzing the temperature series and identifying 'hotspot' areas.

The noted increase in temperature during the rice-growing season across the country is likely to have adverse impacts on rice production. In general, the winter-spring rice season now experiences a warmer climate in many regions of the country (Fig. 9.1). The warming pattern is even more intense for the spring-autumn rice-growing season between June and October/November (Figs. 9.2 and 9.3). Again, the Red River and Mekong River deltas are among the areas with the highest warming rate recorded. Since those two deltas are the primary rice production regions of the country, it is likely that temperature anomalies are already adversely affecting rice production.

4.4. Identifying the potential effect of climate change on agricultural production

4.4.1. The effect of precipitation changes

The trend test results were also mapped together with climate anomalies map and the distribution of agricultural land to identify any potential impacts of climate change on the agricultural sector.

Comparing results of the statistical analysis in Fig. 5 and the visual analysis in Fig. 6, there is a very close connection between the patterns of changes obtained using geostatistical techniques and the results of the Mann-Kendall trend test. Specifically, most of those 'hotspot' areas, where significant changes in precipitation patterns have been identified by geostatistical mapping, have also been further confirmed by the statistical significance of the long-term shifts over time and space. For instance, the north-westernmost regions, the center of the North Central Coast (B-IV), the northern South Central Coast (N-I) and the Central Highlands (N-II) were visually considered as the most prominent areas for precipitation anomalies and, consistent with results of the trend test,

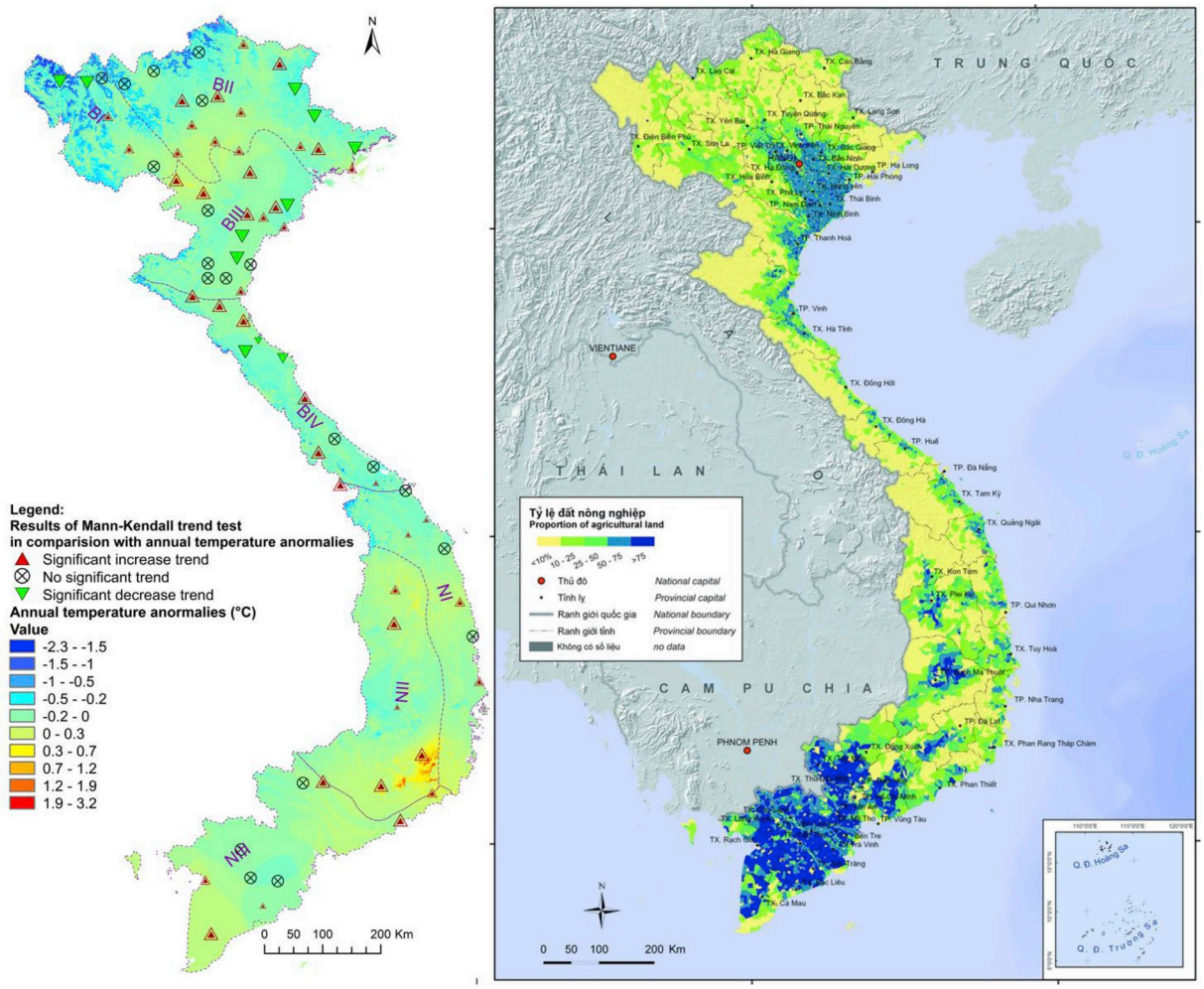

Fig. 11. Results of Mann-Kendall trend test comparing annual mean temperature anomalies *(left)* and the distribution of agricultural land in Vietnam *(right)*.

those locations also show statistically significant evidence of long-term increasing or decreasing precipitation. We can say that there is a robust evidence that Vietnam's climate is changing, not only in certain short periods but also over long historical records of precipitation.

The long-term significant trend in rainfall pattern is identified in areas where there is very high proportion of agricultural land. Specifically, the main farming area in the North is experiencing a significant decline in rainfall whereas the largest agricultural production area of the country in the South is experiencing both significant increases and decreases in rainfall in various locations.

4.4.2. The effect of temperature change

We further analyzed the temperature series by integrating a statistical approach to the outcome graphics of geostatistical techniques and to the land use map (Fig. 11). The outputs of the two approaches are highly correlated from region to region across the country. Most areas with considerably pronounced changes in patterns are also associated with statistically significant long-term trends verified by the Mann-Kendall test. However, no statistically significant change in temperature is identified in the northernmost of the country even though a substantial shift in the pattern is observed in the visual analysis.

Generally, the long-term trends depicted in the findings of both geostatistical mapping and statistical testing used in this study provide important evidence of spatio-temporal changes of climatic conditions throughout Vietnam.

It is evident that most agricultural areas across the country are experiencing a warming pattern in climatic conditions, particularly the two largest rice production areas in the Red River and Mekong River deltas. Many other areas along the coast are also experiencing a long-term increase in temperature which is likely to adversely affect rice production.

5. Conclusions

Changes in climate have been observed across the globe, including in Vietnam. These observed shifts in climate patterns could have adverse impacts on natural systems and human activities such as agricultural production. Our study examined the spatio-temporal trends of climate-related variables and identified the potential detrimental effects on agriculture in Vietnam. Records of monthly precipitation and temperature for a relatively long-term period (1975–2014) over a high density of 112 meteorological stations across the country were used. Combining statistical methods with geostatistical techniques is an effective way to test the statistical significance of trends over time, graphically representing the distribution of climate patterns, and identifying variations and the potential impact on agricultural production.

The findings provide robust evidence of spatio-temporal climate variability and change in Vietnam. The Mann-Kendall trend test confirms the significant long-term trends over time in many regions. The evidence of climate change in Vietnam was further assessed by geostatistical mapping. The visual analysis indicates that rainfall anomalies exhibit a dramatic heterogeneity across regions, in contrast to the ongoing spatially uniform warming in temperature in most parts of the country. The results confirmed that most of the 'hotspot' areas of rainfall and temperature identified by geostatistical mapping have statistically significant long-term changes over time. The findings confirm that ongoing changes in the climate in many areas throughout the country were not only represented by the variations of climatic elements in certain periods, but also by the long-term trends over many years.

Long-term significant trends in rainfall and temperature patterns were identified in areas with very high proportion of agricultural land, particularly for rice production in the Red River and Mekong River deltas. Changes in the rainfall and temperature patterns are very likely to have serious impacts on rice cultivation and productivity during the growing season due to the warming across the country and the surplus or deficit of rainfall in certain areas. It is consequently expected that climate change will have adverse effects on the agricultural sector, including rice production in many regions of Vietnam. Unfavorable climatic conditions could result in increasing frequency and intensity of flooding, water scarcity, and pests and plant diseases, which could lead to lower productivity in rice-growing areas. However, to what extent the changes in climate will affect rice productivity and how farmers will adapt to the changing climate is beyond the scope of this study. Constructing a long-term panel data on climate-related variables and agricultural productivity at a finer scale of spatial aggregation, such as households or communes, is essential to more directly assess the likely impact of climate change on agriculture. While this was not possible to do in the current study, it leaves room for further analysis on climate change impacts and adaptation, which remains of imminent research interest.

Our findings contribute significantly to the understanding of the underlying climate processes and the possible effects of climate change across regions of Vietnam. This evidence-based analysis provides a basis for developing effective climate-related policies to respond to ongoing climate change and to help mitigate the adverse impacts of climate change on human social-economic processes, particularly on agricultural production in rural areas.

Conflicts of interest

None.

Acknowledgments

Parts of the paper have been presented at the 2016 Australian Agricultural and Resource Economics Society (AARES) Annual Conference. We would like to thank discussants and participants for their numerous constructive comments. We would also like to thank Dr. Rhonda Daniels and Dr. Evarn Ooi for their support during the editing process and the Australian Awards for financial support for this work. We are grateful to anonymous reviewers for their constructive feedback and valuable recommendations for the improvement of this manuscript.

Appendix A. Details of homogeneity tests for climate series

Suppose that we have a series of the meteorological variable of a sequence $x_1, x_2 \ldots x_n$ with mean ($\bar{x}$) and standard deviation σ. L is the length of that series and k is likely to be the year of a break or change point.

Standard normal homogeneity test (Alexandersson, 1986)

The test calculates the statistic value T_k by comparing the mean (M) of the first k records with that of the remaining (n-k) records (Jaiswal et al., 2015). k will be considered as a break point if maximizing T_k:

$$T_k = kM_1^2 + (n-k)M_2^2,$$

where M_1 and M_2 are calculated as follows:

$$M_1 = \frac{1}{k}\sum_{i=1}^{k}\frac{(x_i - \bar{x})}{\sigma}$$

$$M_2 = \frac{1}{n-k}\sum_{i=k+1}^{n}\frac{(x_i - \bar{x})}{\sigma}$$

Pettitt's test (Pettitt, 1979)

Consider the two subsamples: $x_1, x_2 \ldots x_t$ and $x_{t+1}, x_{t+2} \ldots x_L$, where t is likely to be the change point. The U_t index is calculated as follows:

$$U_t = \sum_{i=1}^{t}\sum_{j=t+1}^{n} sign(x_t - x_j),$$

$$\text{where: } sign(x_t - x_j) = \begin{cases} 1, \text{ if } (x_t - x_j) > 0 \\ 0, \text{ if } (x_t - x_j) = 0 \\ -1, \text{ if } (x_t - x_j) < 0 \end{cases}$$

If there is a change point t, $|U_t|$ will reach the maximum value K_L at that point:

$$K_L = \max_{1 \le t \le L} |U_t|$$

Then the probability that t is the change point is approximated by (Pettitt, 1979):

$$p = 1 - \exp\left[\frac{-6K_L^2}{L^2 + L^3}\right]$$

Buishand's test (Buishand, 1982)

The cumulative deviation from the mean for *k*th observation of a sequence $x_1, x_2 \ldots x_n$ with mean ($\bar{x}$) is defined as the adjusted partial sum (S):

$$S_k^* = 0 \text{ and } S_k^* = \sum_{i=1}^{k} (x_i - \bar{x}) k = 1, \ldots, n$$

If a series is homogenous with no change point detected, $S_k^* = 0$ because any variation from the mean will fluctuate around that mean. However, if a break exists at *k*th observation in the series, S_k^* will reach a maximum or minimum value and these values could be rescaled to (R) by the standard deviation σ to test for the significance of the change point:

$$R = \left(\max_{0 \le k \le n} S_k^* - \min_{0 \le k \le n} S_k^*\right)/\sigma$$

Von Neumann's test (Wijngaard et al., 2003)

The Von Neumann's test defines the ratio N as the difference between the year-to-year mean square and the variance of data series:

$$N = \frac{\sum_{i=1}^{n-1} (x_i - x_{i-1})^2}{\sum_{i=1}^{n} (x_i - \bar{x})^2}$$

If a series is homogenous, the expected value of N = 2. When there is a break point, N will have a value that is lower than $E(N)$ (Buishand, 1982).

Appendix B. Advantages and limitations of tests for homogeneity

Test for homogeneity	Advantages	Limitations
Pettitt's test (Pettitt, 1979)	– Most commonly used test for change point detection (Jaiswal et al., 2015) – Detect any possible break or change point within the data series (Wijngaard et al., 2003) – Allow detecting the time of the change (Pohlert et al., 2016) Requires no hypothesis about the distribution of the data	– Be suitable for detecting break points in the middle of the data series
Standard normal homogeneity test (Alexandersson, 1986)	– Detect any possible break or change point within the data series (Wijngaard et al., 2003) – More sensitive to any change point at the beginning or the end of that series (Hawkins, 1977; Wijngaard et al., 2003) – Allow detecting the time of the change (Pohlert et al., 2016)	– Require long data series (Alexandersson and Moberg, 1997) – Depend on the distribution assumption of the variables
Buishand's test (Buishand, 1982)	– Detect any possible break or change point within the data series (Wijngaard et al., 2003) – More suitable for detecting break points in the middle of the data series – Use on variables following any type of distribution (Buishand, 1982) – Allow detecting the time of the change (Pohlert et al., 2016)	– Variables need to be independent and identically normally distributed
Neumann's test (Von Neumann, 1941)	– Closely related to the first-order serial correlation (Von Neumann, 1941) – Detecting any possible break or change point within the data series (Wijngaard et al., 2003)	– Do not depend on the distribution assumption of the variables (Vezzoli et al., 2012) – Do not allow detecting the time of the change

Appendix C. List of 112 climate stations in the study

No.	Station name	Longitude	Latitude	No.	Station name	Longitude	Latitude
1	Muong Te	102.5	22.22	29	Chiem Hoa	105.16	22.09
2	Sin Ho	103.14	22.22	30	Ham Yen	105.02	22.04
3	Tam Duong	103.29	22.25	31	Tuyen Quang	105.13	21.49
4	Than Uyen	103.53	21.57	32	Bac Can	105.5	22.09
5	Dien Bien	103.00	21.22	33	Ngan Son	105.59	22.26

6	Lai Chau	103.09	22.04	34	Dinh Hoa	105.38	21.55
7	Tuan Giao	103.25	21.35	35	Thai Nguyen	105.5	21.36
8	Bac Yen	104.25	21.15	36	Phu Ho	105.14	21.27
9	Co Noi	104.09	21.08	37	Viet Tri	105.25	21.18
10	Moc Chau	104.41	20.5	38	Vinh Yen	105.36	21.19
11	Phu Yen	104.38	21.16	39	Bao Lac	105.4	22.57
12	Quynh Nhai	103.34	21.51	40	Cao Bang	106.15	11.4
13	Son La	103.54	21.2	41	Trung Khanh	106.31	22.5
14	Song Ma	103.44	21.04	42	Huu Lung	106.21	21.3
15	Yen Chau	104.18	21.03	43	Lang Son	106.46	21.5
16	Chi Ne	105.47	20.29	44	That Khe	106.28	22.15
17	Hoa Binh	105.2	20.49	45	Bac Giang	106.13	22.18
18	Kim Boi	105.32	20.4	46	Luc Ngan	106.33	21.23
19	Lac Son	105.27	20.27	47	Son Dong	106.51	21.2
20	Mai Chau	105.03	20.39	48	Cua Ong	107.21	21.01
21	Bac Quang	104.52	22.3	49	Tien Yen	107.24	21.2
22	Ha Giang	104.58	22.49	50	Uong Bi	106.45	21.02
23	Bac Ha	104.17	22.32	51	Phu Lien	106.38	20.48
24	Lao Cai	103.58	22.3	52	Ha Dong	105.45	20.58
25	Sa Pa	103.49	22.21	53	Lang	105.51	21.02
26	Luc Yen	104.43	22.06	54	Hai Duong	106.18	20.56
27	MuCangCha	104.03	21.52	55	Hung Yen	106.03	20.39
28	Yen Bai	104.52	21.42	56	Nam Dinh	106.09	20.24
57	Van Ly	106.18	20.07	85	Quang Nam	108.15	15.20
58	Thai Binh	106.21	20.27	86	Quang Ngai	108.48	15.07
59	Nho Quan	105.44	20.20	87	Binh Dinh	109.02	14.31
60	Ninh Binh	105.58	20.14	88	Binh Dinh	109.13	13.46
61	Hoi Xuan	105.07	20.22	89	Phu Yen	109.17	13.05
62	Nhu Xuan	105.34	19.38	90	Khanh Hoa	109.12	12.13
63	Thanh Hoa	105.47	19.45	91	Ninh Thuan	108.59	11.35
64	Tinh Gia	105.47	19.27	92	Binh Thuan	108.06	10.56
65	Yen Dinh	105.40	19.59	93	Kon Tum	108.00	14.3
66	Con Cuong	104.53	19.03	94	Gia Lai	108.01	13.58
67	Do Luong	105.18	18.54	95	Dak Lak	108.03	12.40
68	Quy Chau	105.07	19.34	96	Dak Nong	107.41	12.00
69	Quy Hop	105.09	19.19	97	Lam Dong	107.49	11.32
70	Quynh Luu	105.38	19.10	98	Lam Dong	108.27	11.57
71	Tay Hieu	105.24	19.19	99	Binh Phuoc	106.54	11.32
72	Vinh	105.40	18.40	100	Binh Phuoc	106.59	11.5
73	Ha Tinh	105.54	18.21	101	Tay Ninh	106.07	11.2
74	Huong Khe	105.43	18.11	102	Ba Ria-V.Tau	107.05	10.22
75	Ky Anh	106.17	18.05	103	Long An	105.56	10.47
76	Ba Don	106.25	17.45	104	Tien Giang	106.24	10.21
77	Dong Hoi	106.37	17.29	105	Dong Thap	105.38	10.28
78	Dong Ha	107.05	16.51	106	Tra Vinh	106.12	9.59
79	Khe Sanh	106.44	16.38	107	An Giang	105.08	10.42
80	A Luoi	107.17	16.13	108	Can Tho	105.46	10.02
81	Hue	107.35	16.26	109	Soc Trang	105.58	9.36
82	Nam Dong	107.43	16.10	110	Kien Giang	105.04	10.00
83	Da Nang	108.12	16.02	111	Bac Lieu	105.43	9.17
84	Tam Ky	108.28	15.34	112	Ca Mau	105.09	9.11

Appendix D. Three-stage workflow in data collection and organization, homogenization, and analysis

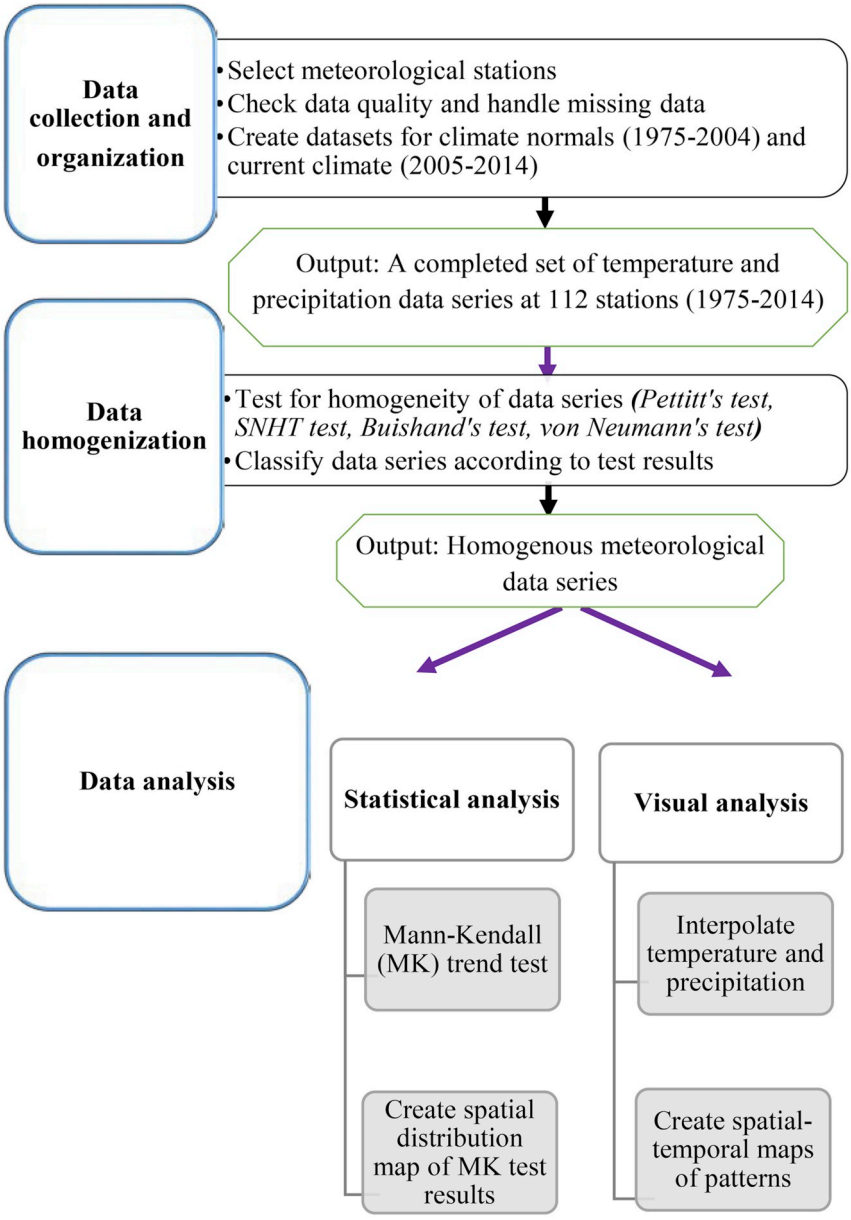
Data collection and organization
•Select meteorological stations
•Check data quality and handle missing data
•Create datasets for climate normals (1975-2004) and current climate (2005-2014)
Output: A completed set of temperature and precipitation data series at 112 stations (1975-2014)
Data homogenization
•Test for homogeneity of data series (Pettitt's test, SNHT test, Buishand's test, von Neumann's test)
•Classify data series according to test results
Output: Homogenous meteorological data series
Data analysis
Statistical analysis
Visual analysis
Mann-Kendall (MK) trend test
Interpolate temperature and precipitation
Create spatial distribution map of MK test results
Create spatial-temporal maps of patterns

References

Alexandersson, H., 1986. A homogeneity test applied to precipitation data. J. Climatol. 6, 661–675. https://doi.org/10.1002/joc.3370060607.

Alexandersson, H., Moberg, A., 1997. Homogenization of Swedish temperature data. Part I: homogeneity test for linear trends. Int. J. Climatol. 17, 25–34. https://doi.org/10.1002/(SICI)1097-0088(199701)17:1<25::AID-JOC103>3.0.CO;2-J.

Arguez, A., Vose, R.S., 2011. The definition of the standard WMO climate normal: the key to deriving alternative climate normals. Bull. Am. Meteorol. Soc. 92, 699–704. https://doi.org/10.1175/2010BAMS2955.1.

Buishand, T.A., 1982. Some methods for testing the homogeneity of rainfall records. J. Hydrol. 58, 11–27. https://doi.org/10.1016/0022-1694(82)90066-X.

Caesar, J., Alexander, L.V., Trewin, B., Tse-ring, K., Sorany, L., Vuniyayawa, V., Keosavang, N., Shimana, A., Htay, M.M., Karmacharya, J., Jayasinghearachchi, D.A., Sakkamart, J., Soares, E., Hung, L.T., Thuong, L.T., Hue, C.T., Dung, N.T.T., Hung, P.V., Cuong, H.D., Cuong, N.M., Sirabaha, S., 2011. Changes in temperature and precipitation extremes over the Indo-Pacific region from 1971 to 2005. Int. J. Climatol. 31, 791–801. https://doi.org/10.1002/joc.2118.

Chen, S., Guo, J., 2017. Spatial interpolation techniques: their applications in regionalizing climate-change series and associated accuracy evaluation in Northeast China. Geomatics, Nat. Hazards Risk 8, 689–705. https://doi.org/10.1080/19475705.2016.1255669.

Conway, D., van Garderen, E.A., Deryng, D., Dorling, S., Krueger, T., Landman, W., Lankford, B., Lebek, K., Osborn, T., Ringler, C., Thurlow, J., Zhu, T., Dalin, C., 2015. Climate and southern Africa's water-energy-food nexus. Nat. Clim. Change 5, 837–846. https://doi.org/10.1038/nclimate2735.

Cressie, N., 2015. Statistics for Spatial Data. John Wiley & Sonshttps://doi.org/10.1002/9781119115151.

Daly, C., Halbleib, M., Smith, J.I., Gibson, W.P., Doggett, M.K., Taylor, G.H., Curtis, J., Pasteris, P.P., 2008. Physiographically sensitive mapping of climatological temperature and precipitation across the conterminous United States. Int. J. Climatol. 28, 2031–2064. https://doi.org/10.1002/joc.1688.

Griffiths, G.M., Chambers, L.E., Haylock, M.R., Manton, M.J., Nicholls, N., Baek, H.J., Choi, Y., Della-Marta, P.M., Gosai, A., Iga, N., Lata, R., Laurent, V., Maitrepierre, L., Nakamigawa, H., Ouprasitwong, N., Solofa, D., Tahani, L., Thuy, D.T., Tibig, L., Trewin, B., Vediapan, K., Zhai, P., 2005. Change in mean temperature as a predictor of extreme temperature change in the Asia–Pacific region. Int. J. Climatol. 25, 1301–1330. https://doi.org/10.1002/joc.1194.

GSO, 2014. General Statistics Office. Available online at: http://gso.gov.vn, Accessed date: 13 May 2016.

Guttman, N.B., 1998. Homogeneity, Data Adjustments and Climatic Normals. National

Climatic Data Center, Asheville, United State Available online at: https://www.stat.washington.edu/peter/7IMSC/Normals.pdf, Accessed date: 17 March 2016.
Hawkins, D.M., 1977. Testing a sequence of observations for a shift in location. J. Am. Stat. Assoc. 72, 180–186. https://doi.org/10.1080/01621459.1977.10479935.
Jaiswal, R.K., Lohani, A.K., Tiwari, H.L., 2015. Statistical analysis for change detection and trend assessment in climatological parameters. Environ. Process. 2, 729–749. https://doi.org/10.1007/s40710-015-0105-3.
Javari, M., 2017. Geostatistical modeling to simulate daily rainfall variability in Iran. Cogent Geosci. 3, 1416877. https://doi.org/10.1080/23312041.2017.1416877.
Johnston, K., Ver Hoef, J.M., Krivoruchko, K., Lucas, N., 2001. Using ArcGIS Geostatistical Analyst. Esri Redlands Available online at: http://dusk2.geo.orst.edu/gis/geostat_analyst.pdf, Accessed date: 17 June 2016.
Jones, D.A., Wang, W., Fawcett, R., 2009. High-quality spatial climate data-sets for Australia. Aust. Meteorol. Oceanogr. J. 58, 233. https://doi.org/10.22499/2.5804.003.
Journel, A.G., Huijbregts, C.J., 1978. Mining Geostatistics. Academic Press Available online at: https://trove.nla.gov.au/version/44967529, Accessed date: 27 May 2016.
Kendall, M.G., 1962. Rank Correlation Methods. Griffin, Oxford, England.
Kundu, S., Khare, D., Mondal, A., Mishra, P.K., 2015. Analysis of spatial and temporal variation in rainfall trend of Madhya Pradesh, India (1901–2011). Environ. Earth Sci. 73, 8197–8216. https://doi.org/10.1007/s12665-014-3978-y.
Lau, K.M., Yang, S., 1997. Climatology and interannual variability of the southeast Asian summer monsoon. Adv. Atmos. Sci. 14, 141–162. https://doi.org/10.1007/s00376-997-0016-y.
Longobardi, A., Villani, P., 2010. Trend analysis of annual and seasonal rainfall time series in the Mediterranean area. Int. J. Climatol. 30, 1538–1546. https://doi.org/10.1002/joc.2001.
Mann, H.B., 1945. Nonparametric tests against trend. Econometrica 13, 245–259. https://doi.org/10.2307/1907187.
Meshram, S.G., Singh, V.P., Meshram, C., 2016. Long-term trend and variability of precipitation in Chhattisgarh State, India. Theor. Appl. Climatol. 1–16. https://doi.org/10.1007/s00704-016-1804-z.
Moral, F.J., 2010. Comparison of different geostatistical approaches to map climate variables: application to precipitation. Int. J. Climatol. 30, 620–631. https://doi.org/10.1002/joc.1913.
Mustafa, G., Bilal, C., Hikmet, G., 2007. Assessment of some spatial climatic layers through GIS and statistical analysis techniques in Samsun Turkey. Meteorol. Appl. 14, 163–169. https://doi.org/10.1002/met.18.
Nam, W.-H., Hong, E.-M., Baigorria, G.A., 2016. How climate change has affected the spatio-temporal patterns of precipitation and temperature at various time scales in North Korea. Int. J. Climatol. 36, 722–734. https://doi.org/10.1002/joc.4378.
Nelson, G.C., Rosegrant, M.W., Koo, J., Robertson, R., Sulser, T., Zhu, T., Ringler, C., Msangi, S., Palazzo, A., Batka, M., 2009. Climate change: impact on agriculture and costs of adaptation. Int. Food Policy Res. Inst. https://doi.org/10.2499/0896295354.
Nguyen, D.Q., Renwick, J., McGregor, J., 2013. Variations of surface temperature and rainfall in Vietnam from 1971 to 2010. Int. J. Climatol. https://doi.org/10.1002/joc.3684.
Nguyen, T.D., Uvo, C., Rosbjerg, D., 2007. Relationship between the tropical Pacific and Indian Ocean sea-surface temperature and monthly precipitation over the central highlands, Vietnam. Int. J. Climatol. 27, 1439–1454. https://doi.org/10.1002/joc.1486.
Ninyerola, M., Pons, X., Roure, J.M., 2000. A methodological approach of climatological modeling of air temperature and precipitation through GIS techniques. Int. J. Climatol. 20, 1823–1841. https://doi.org/10.1002/1097-0088(20001130)20:14<1823::AID-JOC566>3.0.CO;2-B.
Pardo-Igúzquiza, E., 1998. Comparison of geostatistical methods for estimating the areal average climatological rainfall mean using data on precipitation and topography. Int. J. Climatol. 18, 1031–1047. https://doi.org/10.1002/(SICI)1097-0088(199807)18:9<1031::AID-JOC303>3.0.CO;2-U.
Pettitt, A.N., 1979. A non-parametric approach to the change-point problem. J. R. Stat. Soc. Ser. C (Appl. Stat.) 28, 126–135. https://doi.org/10.2307/2346729.
Pil, K., 2013. Spatial data process using Python script and visual programming language in ArcGIS. Comput. Technol. Appl. 4 (2013), 275–283.
Pingale, S.M., Khare, D., Jat, M.K., Adamowski, J., 2014. Spatial and temporal trends of mean and extreme rainfall and temperature for the 33 urban centers of the arid and semi-arid state of Rajasthan, India. Atmos. Res. 138, 73–90. https://doi.org/10.1016/j.atmosres.2013.10.024.
Pohlert, T., Pohlert, M.T., Kendall, S., 2016. Package 'trend'. Available online at: https://cran.r-project.org/web/packages/trend/trend.pdf, Accessed date: 11 March 2016.
Portmann, R.W., Solomon, S., Hegerl, G.C., 2009. Spatial and seasonal patterns in climate change, temperatures, and precipitation across the United States. Proc. Natl. Acad. Sci. Unit. States Am. 106, 7324–7329. https://doi.org/10.1073/pnas.0808533106.
Prudhomme, C., Reed, D.W., 1999. Mapping extreme rainfall in a mountainous region using geostatistical techniques: a case study in Scotland. Int. J. Climatol. 19, 1337–1356. https://doi.org/10.1002/(SICI)1097-0088(199910)19:12<1337::AID-JOC421>3.0.CO;2-G.
Río, S.d., Herrero, L., Fraile, R., Penas, A., 2011. Spatial distribution of recent rainfall trends in Spain (1961–2006). Int. J. Climatol. 31, 656–667. https://doi.org/10.1002/joc.2111.
Rosenzweig, C., Iglesias, A., Yang, X., Epstein, P.R., Chivian, E., 2001. Climate change and extreme weather events; implications for food production, plant diseases, and pests. Global Change Hum. Health 2, 90–104. Available online at: https://digitalcommons.unl.edu/nasapub/24, Accessed date: 11 March 2016.
Rulfová, Z., Kyselý, J., 2013. Disaggregating convective and stratiform precipitation from station weather data. Atmos. Res. 134, 100–115. https://doi.org/10.1016/j.atmosres.2013.07.015.
Sayemuzzaman, M., 2014. Spatio-temporal Trends of Climate Variability in North Carolina. North Carolina Agricultural and Technical State University, ProQuest Dissertations Publishing.
Stocker, T.F., Qin, D., Plattner, G.-K., Tignor, M., Allen, S.K., Boschung, J., Nauels, A., Xia, Y., Bex, V., Midgley, P.M., 2014. Climate Change 2013: the Physical Science Basis. Cambridge University Press, Cambridge, UK, and New York Available online at: www.cambridge.org/9781107661820, Accessed date: 17 January 2017.
Thomas, T., Christiaensen, L., Do, Q.T., Trung, L.D., 2010. Natural Disasters and Household Welfare: Evidence from Vietnam, Policy Research Working Paper Series. World Bank.
UNEP, 2009. Vietnam Assessment Report on Climate Change. Institute of Strategy and Policy on Natural Resources and Environment, Van hoa - Thong tin Publishing House, pp. 127.
USEPA, 2016. Climate Change Indicators in the United States, 2016, fourth ed. Available online at: www.epa.gov/climate-indicators, Accessed date: 25 March 2016 EPA 430-R-16-004.
VAAS, 2010. Rice Production in Vietnam. Vietnam Academy of Agricultural Sciences.
Vezzoli, R., Pecora, S., Zenoni, E., Tonelli, F., 2012. Data Analysis to Detect Inhomogeneity, Change Points, Trends in Observations: an Application to Po River Discharge Extremes. CMCC Research Paper. https://doi.org/10.2139/ssrn.2195345.
Viola, F., Liuzzo, L., Noto, L.V., Lo Conti, F., La Loggia, G., 2014. Spatial distribution of temperature trends in Sicily. Int. J. Climatol. 34, 1–17. https://doi.org/10.1002/joc.3657.
VNGP, 2011. The National Strategy on Climate Change. Vietnam Government Portal Available online at: http://chinhphu.vn, Accessed date: 12 March 2015.
Von Neumann, I., 1941. Distribution of the ratio of the mean square successive difference to the variance. Ann. Math. Statist. 12, 367–395. https://doi.org/10.1214/aoms/1177731677.
Wijngaard, J.B., Klein Tank, A.M.G., Können, G.P., 2003. Homogeneity of 20th century European daily temperature and precipitation series. Int. J. Climatol. 23, 679–692. https://doi.org/10.1002/joc.906.
Xu, M., Kang, S., Wu, H., Yuan, X., 2018. Detection of spatio-temporal variability of air temperature and precipitation based on long-term meteorological station observations over Tianshan Mountains, Central Asia. Atmos. Res. 203, 141–163. https://doi.org/10.1016/j.atmosres.2017.12.007.
Zarenistanak, M., Dhorde, A.G., Kripalani, R.H., 2014. Trend analysis and change point detection of annual and seasonal precipitation and temperature series over southwest Iran. J. Earth Syst. Sci. 123, 281–295. https://doi.org/10.1007/s12040-013-0395-7.
Zhao, G., Siebert, S., Enders, A., Rezaei, E.E., Yan, C., Ewert, F., 2015. Demand for multi-scale weather data for regional crop modeling. Agric. For. Meteorol. 200, 156–171. https://doi.org/10.1016/j.agrformet.2014.09.026.